

1 Fully Specified Estimation Plan for
2 Optimal Static Parametric Estimation of Arbitrary Distributions
3 (OSPEAD)
4 *Public Version*

5 Rucknium

6 November 18, 2022

7 **1 Introduction**

8 Research on Monero and similar systems has established the vital importance of constructing a decoy selection
9 algorithm that closely resembles the real spend age distribution. A sample of researchers' conclusions and recom-
10 mendations follows:

11 As we have seen the current [2017] sampling strategy for mix-ins fails drastically in preventing temporal
12 analysis. There are two possible strategies towards mitigating the ensuing risks: (a) mimic users'
13 spending behavior or, (b) force mix-ins to be picked according to some "unknown" distribution.

14 - [Kumar et al., 2017]

15 We have provided evidence that the strategy by which Monero mixins are sampled [circa 2017] results in
16 a different time distribution than real spends, significantly undermining the untraceability mechanism.
17 To correct this problem, the mixins should ideally be sampled in such a way that the resulting time
18 distributions match.

19 - [Möser et al., 2018]

20 The mixin sampling distribution has since been replaced with a gamma distribution (from [Möser et al., 2018])
21 fitted to the empirical spend-time distribution. Our results show that these sampling distribution changes
22 have made a significant impact in reducing the accuracy of the guess-newest heuristic.

23 - [Ye et al., 2020]

24 [A mimicking decoy selection algorithm's] anonymity depends on how well $\hat{\mathcal{S}}$ [the decoy selection al-
25 gorithm] estimates \mathcal{S} [the real spend age distribution]....It is therefore reasonable to expect that if the
26 mimicking sampler has access to the true source distribution \mathcal{S} , its anonymity should be close to optimal.
27 In the following, we give an [sic] evidence that this is the case.

28 - [Ronge et al., 2021]

29 The problem of creating a decoy selection algorithm that minimizes the usefulness of timing information to an
30 adversary was recognized by the Monero Research Lab very early [Mackenzie et al., 2015]:

31 One solution to this problem is to determine a non-uniform method of choosing transaction outputs
32 for ring signatures; choose transaction outputs based on their age such that the probability that these
33 outputs are chosen for a ring signature is inversely related to the probability that they have been
34 spent already. This would suggest that we, the developers of Monero, must estimate the probability
35 distribution governing the age of transaction outputs.

36 A reliable estimator of the real spend age probability distribution has been elusive. [Möser et al., 2018] estimated
37 the distribution based on partial knowledge of real spends obtained from other de-anonymization techniques. The
38 introduction of RingCT and other improvements to Monero have rendered the de-anonymization techniques of
39 [Möser et al., 2018] ineffective ([Ye et al., 2020], [Vijayakumaran, 2021]). Therefore, an updated and improved es-
40 timate would require an estimator to use only the fully anonymized ring data on the Monero blockchain.

41 In this document I lay out such an estimator and justify it in a fairly rigorous manner.

42 Part I

43 Undisclosed Portion [Withheld]

⁴⁴ **Part II**

⁴⁵ **Disclosed Portion**

⁴⁶ **2 Plain English Explanation of the Problem**

⁴⁷ **2.1 Timing Metadata in Monero Transactions**

⁴⁸ Through great effort, Monero researchers and software developers have been able to conceal most information about
⁴⁹ transactions even though all Monero nodes share the blockchain database itself. However, transactions still contain
⁵⁰ some information that distinguishes them from one another.

⁵¹ One key piece of information embedded in each Monero transaction is the time that it was confirmed in a mined
⁵² block. Timestamps are an inherent property of blockchain-based cryptocurrencies. The timestamp ensures that
⁵³ coins are not double-spent.

⁵⁴ Each Monero transaction creates at least two *outputs*, which are amounts of Monero that can be spent in a
⁵⁵ subsequent transaction. When a user that has received an output wishes to spend it, the wallet software he or she
⁵⁶ uses will include that output in the set of outputs within the ring signature. Monero's current ring size is 16, so
⁵⁷ there will be 15 *decoy* outputs listed in the ring and 1 *real spend* output.

Table 1: Ring Members of Transaction 8bc3b73e48881d48cd69f1bf82a06b6a7b94bfd0dbf85edac535dab9270a305b

Output Public Key	Block Number	Block Timestamp
033a3d4b817bfaba6472f249fdb0dc6b00ecfe20983cea5e608fe5e679b0d23b	2666408	2022-07-13 13:27:42
866c4cf39af3e8785cbda21a9cbaa120424df76d5d05518d3ec888b94acf4c2b	2683943	2022-08-06 20:03:35
c8c3f8660776fad9dee0dd9bd6a3e02f52ba5e4b4785419db7a4131f1d1aa1ff	2692667	2022-08-19 02:10:18
ca2f709c371c21a8ab33cddab4b593c24dd52b0ca9e4835ddcbc1f7f0b38e8c7	2696371	2022-08-24 06:06:50
1f11eb618ad7bb9a26a436af1190532c3744d0c0c3b335b6d3fd65b0a9911585	2697585	2022-08-25 21:24:57
6cd9e83b9f75e44a00310aec8935954a23bcdfa34c4fb5aa5e177212fd45ce95	2698303	2022-08-26 22:06:16
9ab87cffbc8eb76a0affbc9d004967ba1ca1ab008ebe68444d687a5d5a1cb145	2698869	2022-08-27 15:36:55
52ae53b9b67316c932db550c386fa7092952d65f9a9d52e261dc0f6ccba78c0	2699496	2022-08-28 12:52:01
19357e641d525fd001945d87829045e3ac6ad829ca92c90b729f152e7dc86b4a	2699840	2022-08-29 00:34:55
2bcdcb2b0b656cefefec925cbe122ecc0bb3d83bf61dfa0ac5a6c96a586ea0560	2699843	2022-08-29 00:39:49
56672f13802cca5363cd5def25c9af4be5ad2e625401d6381568902dca5b0b35	2700102	2022-08-29 09:31:16
bbae1b9ca63e017d030e295a5c9f92ed13152c82a32fdc10458912b9e0fc4e1a	2700241	2022-08-29 14:12:24
cc94142537e87fb36713c84c2bf8465bde03f442d155391025e078bac2154cef	2700606	2022-08-30 02:04:45
dda4c8f4c51b387e03b5ce97b187a5ccb4fb03ea622c62de5afb698f0351215	2700755	2022-08-30 06:59:12
846717c3b56dcf2c87a92b71890fdde13c72081d8d7e40ddbcba2e82d866c063	2700908	2022-08-30 12:10:55
6241dc9af536fd23584c11b6a9c84c9fd692fc5dbc9326741db6dde3f05832e2	2700918	2022-08-30 12:33:33

Source: <https://xmrchain.net/tx/8bc3b73e48881d48cd69f1bf82a06b6a7b94bfd0dbf85edac535dab9270a305b>

⁵⁸ The timestamp of all of those outputs in a ring is available to anyone running a full Monero node or even
⁵⁹ someone who knows how to use a web-based Monero block explorer. Table 1 contains an example of a ring with
⁶⁰ the time stamps of each ring member. Timing information is not the only data that is available to external
⁶¹ observers of the Monero blockchain, but the timing data presents special challenges. Over a year, there will be
⁶² about $30 \cdot 24 \cdot 365 = 262,800$ different timestamps (each timestamp corresponding to a unique block on the Monero
⁶³ blockchain). Since the number of timestamp values is so large compared to the number of decoys, timing information
⁶⁴ can help an anti-privacy adversary possibly narrow down which ring member is the real spend.

⁶⁵ Other types of data on the blockchain cannot take so many values in practice. The number of outputs of a
⁶⁶ transaction are limited to 16. Currently the maximum number of inputs of a transaction is about 146, but in practice

the vast majority of transactions have fewer than 5 inputs.¹ Therefore, the amount of information contained in timestamp data dwarfs the information from the number of inputs or outputs of a transaction. Transaction fee and the `tx_extra` field in theory could have many distinguishing values. In practice, the “official” reference wallet software allows users to set one of only 4 fee priority levels and restricts the format of data in the `tx_extra` field. The difference between the timing data and other types of observable data in a Monero transaction is similar to the difference between data on a person’s birth date and race. Birth date reveals much more information than race since it can take so many values. Race can only be a pretty limited set of values. For an in-depth discussion of metadata available to Monero blockchain observers, see [Krawiec-Thayer et al., 2021].

2.2 Decoys Must Be Credible

The core challenge of decoys is intuitive: Like decoys in all contexts, a decoy only serves its purpose if — to observers — it looks like the real thing. Unfortunately, previous versions of Monero did a poor job of selecting decoys that looked like the real thing. According to one estimate, 80 percent of Monero transactions prior to February 2017 could be traced simply by guessing that the youngest ring member was the real spend because selected decoys tended to be much older than the real spends ([Möser et al., 2018]). Monero’s decoy selection algorithm has been changed in recent years to correct flaws found by existing research, but there is still a lot of room for improvement.

To explain the problem I will use the extreme case of what can happen if a given real spend has zero decoys nearby in the timestamp distribution. Monero’s actual decoy selection algorithm does not suffer from this extreme flaw, but it serves its purpose as an introduction to the issue.

Figure 1: Adequate Decoy Selection Algorithm

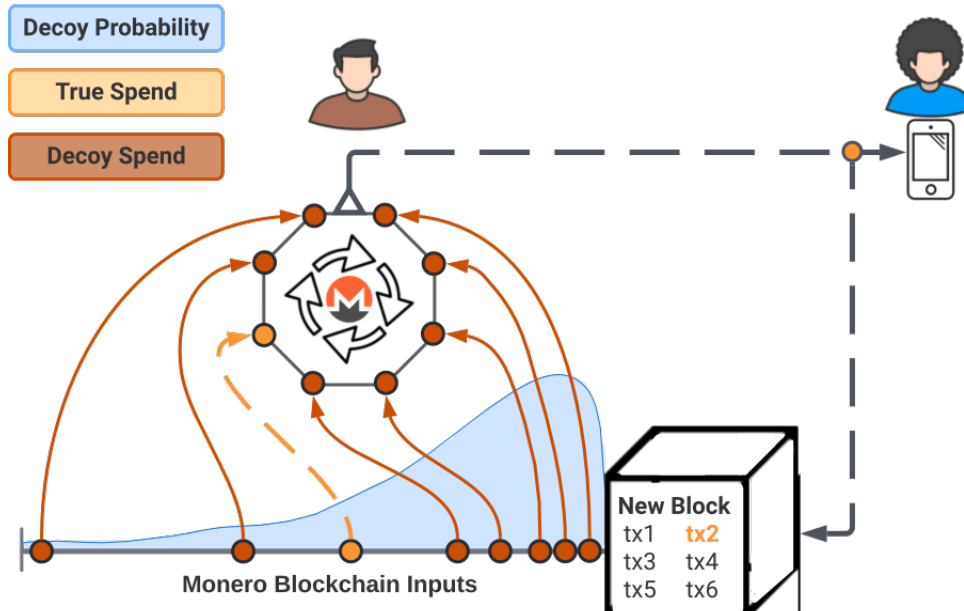


Image designed by ACK-J (<https://github.com/ack-j>)

The height of the blue shape in Figure 1 represents the probability that the decoy selection algorithm selects outputs as decoys from certain blockchain time stamps. Younger outputs are more likely to be selected as decoys since younger outputs are also more likely to be the real spends. Since there is a high probability that a decoy (red circle) could be selected from the same time interval as the real spend (orange), it is difficult for an anti-privacy adversary to deduce that the orange circle is the real spend.

¹See discussion: <https://libera.monerologs.net/monero-dev/20220526>

90 Figure 2 shows what would happen if the decoy selection algorithm were severely defective. There is a portion
 91 of the age distribution that the decoy selection algorithm will never select from. The height of the blue shape is
 92 zero at that interval. In this hypothetical, the fact that no decoy would be selected in that interval would be known
 93 by an anti-privacy adversary since the decoy selection algorithm is written into Monero’s public open source code,
 94 at least for Monero wallets that are open source. Therefore, there would be a 100 percent probability that the ring
 95 member selected in that interval was the real spend. This particular transaction would be 100 percent traceable.
 96 To repeat, this is the extreme case that does not happen in practice. The current decoy selection algorithm is not
 97 severely defective like this hypothetical example, but it has significant shortcomings.

Figure 2: Defective Decoy Selection Algorithm

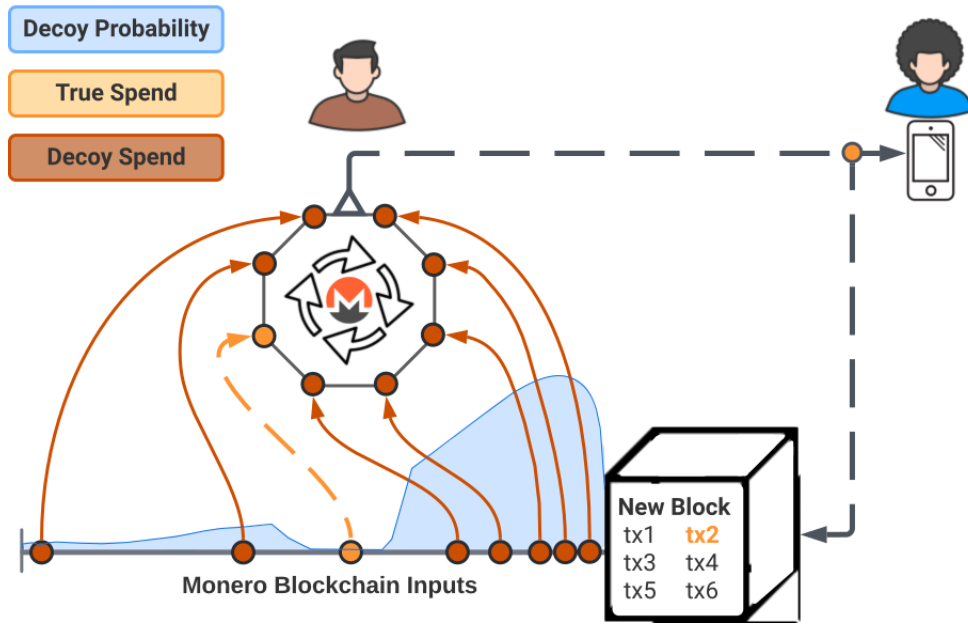


Image designed by ACK-J (<https://github.com/ack-j>)

98 The ideal decoy selection algorithm would select decoys from every point on the age distribution in exact
 99 proportion to the real spends. For a ring size of 16, this ideal algorithm would provide 15 decoys of “camouflage”
 100 on top of every real spend across the entire age distribution. In ideal circumstances, such an algorithm would
 101 not give any hint about the real spend to an anti-privacy adversary. The best an adversary could do is random
 102 guessing about the real spend, which would only achieve a success rate of $1/16 = 6.25\%$. The “defective” algorithm
 103 described above provided zero decoys in a certain age interval, which would lead to full traceability of transactions
 104 that spend outputs that were a certain age. Monero’s current decoy selection algorithm lies somewhere between the
 105 two extremes of ideal and severely defective. The goal of OSPEAD is to move the decoy selection algorithm much
 106 closer to the ideal shape.

107 3 The Solution

108 The goal of OSPEAD is to use a special type of mathematical function called a parametric probability density
 109 function to match the real spend age distribution as closely as possible. The close match will provide about 15
 110 decoys for every real spend along nearly every interval of the age distribution. The match cannot be perfect, however.
 111 Parametric probability density functions can only serve as an approximation of complex real human behavior.

112 There are only a limited number of decoys available per ring. Therefore, if more decoy “camouflage” is moved
 113 from section A to section B on the age distribution, users who happen to spend outputs of an age that falls into

section A will experience a reduction in privacy; users spending from section B will experience an increase in privacy. Therefore with the imperfect parametric probability distribution functions there is an unavoidable trade-off. The terms of the trade-off can be made precise mathematically, but the correct choice of trade-off is a judgment call.

Given that the “correct” trade-off is a judgment call, OSPEAD involves a procedure to obtain the best decoy selection algorithm under several different sets of criteria. Once these candidate algorithms are determined, a single best algorithm will be selected though a judgment call. In the next section I describe the proposed sets of criteria: privacy impoverishment, economic welfare, inequality minimization, worst-case-scenario minimization, Maximum Likelihood Estimation, and maximize resistance to a specific attack.

4 Criteria for Best Fit

At first glance constructing $f_D(x)$, the probability density function (PDF) of the decoy selection algorithm, appears to be a standard problem: Extract the real spend age distribution $f_S(x)$ “data” through some method and then fit some distribution to it in order to form $f_D(x)$. Typically in applied statistical work, “fitting some distribution” would be done via nonparametric means or Maximum Likelihood Estimation (MLE) for a parametric approach. Since we are setting aside nonparametric methods in the short term, MLE may see like the way forward.

I would argue instead that what we confront here is not actually a standard problem, despite appearances. An MLE approach, which is the approach taken in [Möser et al., 2018], may make sense if what we are interested in is conducting hypothesis tests on the parameters of parametric distribution families, a typical scientific exercise. In fact, MLE is quite good at that task, assuming certain crucial assumptions are met, since asymptotically it is usually guaranteed to achieve minimum variance among unbiased estimators.

What we are trying to do here with construction of $f_D(x)$ has little to do with conducting hypothesis tests, however. Most statistical methods are interested in separating statistical signal from noise. What we are trying to do is quite the opposite: merge the signal (real spends) and noise (decoys) so that even a determined and sophisticated statistician cannot distinguish them. We are not trying to minimize variance in fitting $f_D(x)$ to $f_S(x)$. Rather, we are trying to minimize risk to user privacy. We are trying to minimize traceability of Monero transactions. This goal requires us to be more creative in our approach.

In general, our goal is to “cover” every age interval with 15 decoys for every real spend that comes from that interval. A user who spends from a point of the age distribution that is not covered by at least 15 decoys experiences a privacy deficit. A user who spends from a point of the age distribution that is covered by more than 15 decoys has a surplus of decoys. To approach the ideal of all users being protected by a single-hop anonymity set of 16, we can move these decoys from the surplus at particular age x values to the x values with deficits. I will build OSPEAD around the idea of minimizing this privacy deficit for all x , defined as $h(x) = \max\{0, f_S(x) - f_D(x)\}$. I also include a symmetric option: $h_{sym}(x) = |f_S(x) - f_D(x)|$ as a possible minimization objective.

To justify my proposed methodology, I will quote extensively from the second edition of *Statistical Inference* by George Casella & Roger L. Berger ([Casella & Berger, 2002]). In the book’s preface, the authors write, “The purpose of this book is to build theoretical statistics (as different from mathematical statistics) from the first principles of probability theory....The book is intended for first-year graduate students majoring in statistics or in a field where a statistics concentration is desirable.” As far as I can tell, it is widely used for that purpose, at least within economics. For example, the first course in the econometrics sequence of MIT’s economics doctoral program uses the book as its primary textbook.² Therefore, in my view the book is authoritative enough to lean on in justifying my proposed approach.

I will begin by quoting from pages 348–350:

²<https://ocw.mit.edu/courses/economics/14-381-statistical-method-in-economics-fall-2018/syllabus/>

Other economics doctoral programs likely do as well, but we cannot know for sure since many of them keep their syllabi hidden behind student login screens.

155 *7.3.4 Loss Function Optimality*

156 Our evaluations of point estimators have been based on their mean squared error performance. Mean
157 squared error is a special case of a function called a *loss function*. The study of the performance, and
158 the optimality, of estimators evaluated through loss functions is a branch of *decision theory*.

159 After the data $\mathbf{X} = \mathbf{x}$ are observed, where $\mathbf{X} \sim f(\mathbf{x}|\theta)$, $\theta \in \Theta$, a decision regarding θ is made. The set of
160 allowable decisions is the *action space*, denoted by \mathcal{A} . Often in point estimation problems \mathcal{A} is equal to
161 Θ , the parameter space, but this will change in other problems (such as hypothesis testing—see Section
162 8.3.5).

163 The loss function in a point estimation problem reflects the fact that if an action a is close to θ , then
164 the decision a is reasonable and little loss is incurred. If a is far from θ , then a large loss is incurred.
165 The loss function is a nonnegative function that generally increases as the distance between a and θ
166 increases. If θ is real-valued, two commonly used loss functions are

$$\text{absolute error loss, } L(\theta, a) = |a - \theta|,$$

167 and

$$\text{squared error loss, } L(\theta, a) = (a - \theta)^2.$$

168 Both of these loss functions increase as the distance between θ and a increases, with minimum value
169 $L(\theta, \theta) = 0$. That is, the loss is minimum if the action is correct. Squared error loss gives relatively more
170 penalty for large discrepancies, and absolute error loss gives relatively more penalty for small discrepancies.
171 A variation of squared error loss, one that penalizes overestimation more than underestimation,
172 is

$$L(\theta, a) = \begin{cases} (a - \theta)^2 & \text{if } a < \theta \\ 10(a - \theta)^2 & \text{if } a \geq \theta. \end{cases} \quad (1)$$

173 A loss that penalizes errors in estimation more if θ is near 0 than if $|\theta|$ is large, a relative squared error
174 loss, is

$$L(\theta, a) = \frac{(a - \theta)^2}{|\theta| + 1}.$$

175 Notice that both of these last variations of squared error loss could have been based instead on ab-
176 solute error loss. **In general, the experimenter must consider the consequences of various**
177 **errors in estimation for different values of θ and specify a loss function that reflects these**
178 **consequences.** [my emphasis]

179 In a loss function or *decision theoretic* analysis, the quality of an estimator is quantified in its *risk*
180 *function*; that is, for an estimator $\delta(\mathbf{x})$ of θ , the risk function, a function of θ , is

$$R(\theta, \delta) = E_\theta L(\theta, \delta(\mathbf{X})). \quad (2)$$

181 At a given θ , the risk function is the average loss that will be incurred if the estimator $\delta(\mathbf{x})$ is used.

182 Since the true value of θ is unknown, we would like to use an estimator that has a small value of $R(\theta, \delta)$
183 for all values of θ . This would mean that, regardless of the true value of θ , the estimator will have a
184 small expected loss. If the qualities of two different estimators, δ_1 and δ_2 , are to be compared, then they
185 will be compared by comparing their risk functions, $R(\theta, \delta_1)$ and $R(\theta, \delta_2)$. If $R(\theta, \delta_1) < R(\theta, \delta_2)$ for all
186 $\theta \in \Theta$, then δ_1 is the preferred estimator because δ_1 performs better for all θ . More typically, the two
187 risk functions will cross. Then the judgment as to which estimator is better may not be so clear-cut.

188 The risk function for an estimator δ is the expected loss, as defined in (2). For squared error loss, the
189 risk function is a familiar quantity, the mean squared error (MSE) that was used in Section 7.3.1. There
190 the MSE of an estimator was defined as $\text{MSE}(\theta) = E_\theta(\delta(\mathbf{X}) - \theta)^2$, which is just $E_\theta L(\theta, \delta(\mathbf{X})) = R(\theta, \delta)$
191 if $L(\theta, a) = (a - \theta)^2$. As in Chapter 7 we have that, for squared error loss,

$$R(\theta, \delta) = \text{Var}_\theta \delta(\mathbf{X}) + (\text{E}_\theta \delta(\mathbf{X}) - \theta)^2 = \text{Var}_\theta \delta(\mathbf{X}) + (\text{Bias}_\theta \delta(\mathbf{X}))^2.$$

This risk function for squared error loss clearly indicates that a good estimator should have both a small variance and a small bias. A decision theoretic analysis would judge how well an estimator succeeded in simultaneously minimizing these two quantities.

It would be an atypical decision theoretic analysis in which the set \mathcal{D} of allowable estimators was restricted to the set of unbiased estimators, as was done in Section 7.3.2. [my emphasis] Then, minimizing the risk would just be minimizing the variance. A decision theoretic analysis would be more comprehensive in that both the variance and bias are in the risk and will be considered simultaneously. An estimator would be judged good if it had a small, but probably nonzero, bias combined with a small variance.

The text then goes into several specific examples of risk analysis and then briefly explores risk within a Bayesian framework. What does Section 7.3.2 (page 334), referenced above, say?

7.3.2 Best Unbiased Estimators

As noted in the previous section, a comparison of estimators based on MSE considerations may not yield a clear favorite. Indeed, there is no one “best MSE” estimator. Many find this troublesome or annoying, and rather than doing MSE comparisons of candidate estimators, they would rather have a “recommended” one.

The reason that there is no one “best MSE” estimator is that the class of all estimators is too large a class. (For example, the estimator $\hat{\theta} = 17$ cannot be beaten in MSE at $\theta = 17$ but is a terrible estimator otherwise.) One way to make the problem of finding a “best” estimator tractable is to limit the class of estimators. A popular way of restricting the class of estimators, the one we consider in this section, is to consider only unbiased estimators.

If W_1 and W_2 are both unbiased estimators of a parameter θ , that is, $\text{E}_\theta W_1 = \text{E}_\theta W_2 = \theta$, then their mean squared error are equal to their variances, so we should choose the estimator with the smaller variance. If we can find an unbiased estimator with uniformly smallest variance—a best unbiased estimator—then our task is done.

[Casella & Berger, 2002] then go on to give a formal definition of best unbiased estimator — also known as uniform minimum variance unbiased estimator (UMVUE) — in Definition 7.3.7 and then give the Cramér–Rao Lower Bound (CRLB) in Theorem 7.3.9 and Corollary 7.3.10. Corollary 7.3.15 is also useful. The gist of the discussion is that certain unbiased estimators of a parameter θ (the text uses the notation $\tau(\theta)$, with τ being some continuous function of θ , in order to be more general) of a distribution $f(\mathbf{x}|\theta)$ may achieve the lowest variance possible in this setting: the Cramér–Rao Lower Bound (CRLB).

Now I will move on to examining Maximum Likelihood Estimation (MLE) in this entire context. First I will reference the definition of asymptotic variance from [Casella & Berger, 2002], page 471. Let k_n be some normalizing constant.

Definition 10.1.9 For an estimator T_n , suppose that $k_n(T_n - \tau(\theta)) \rightarrow n(0, \sigma^2)$ in distribution. The parameter σ^2 is called the *asymptotic variance* or *variance of the limit distribution* of T_n .

I also need their definition of asymptotic efficiency to make my point:

Definition 10.1.11 A sequence of estimators W_n is asymptotically efficient for a parameter $\tau(\theta)$ if $\sqrt{n}[W_n - \tau(\theta)] \rightarrow n[0, v(\theta)]$ in distribution and

$$v(\theta) = \frac{[\tau'(\theta)]^2}{\text{E}_\theta \left(\left(\frac{\partial}{\partial \theta} \log f(X|\theta) \right)^2 \right)};$$

that is, the asymptotic variance of W_n achieves the Cramér–Rao Lower Bound.

232 Finally, we come to one of the primary reasons MLE is so popular in applied statistical work:

233 **Theorem 10.1.12 (Asymptotic efficiency of MLEs)** Let X_1, X_2, \dots , be iid $f(x|\theta)$, let $\hat{\theta}$ denote
 234 the MLE of θ , and let $\tau(\theta)$ be a continuous function of θ . Under the regularity conditions in Miscellanea
 235 10.6.2 on $f(x|\theta)$ and, hence $L(\theta, \mathbf{x})$ [this expression, the likelihood function, is defined in Theorem 10.1.6
 236 as $L(\theta|\mathbf{x}) = \prod_{i=1}^n f(x_i|\theta)$],

$$\sqrt{n} [\tau(\hat{\theta}) - \tau(\theta)] \rightarrow n [0, v(\theta)],$$

237 where $v(\theta)$ is the Cramér–Rao Lower Bound. That is, $\tau(\hat{\theta})$ is a consistent and asymptotically efficient
 238 estimator of $\tau(\theta)$.

239 Later, at the top of page 477, [Casella & Berger, 2002] make this comment:

240 Since the MLE is typically asymptotically efficient, another estimator cannot hope to beat its asymptotic
 241 variance. However, other estimators may have other desirable properties (ease of calculation, **robust-**
 242 **ness to underlying assumptions** [my emphasis]) that make them desirable. In such situations, the
 243 efficiency of the MLE becomes important in calibrating what we are giving up if we use an alternative
 244 estimator.

245
 246 Let us break down what [Casella & Berger, 2002] are saying in these passages, and how they relate to OSPEAD.
 247 They set up a framework for decision-making based on statistical analysis. Loss functions, decision theory, and risk
 248 functions are the main elements of this framework. They then discuss some of the most common loss functions,
 249 Mean Squared Error (MSE) being one of them. I note in passing that they discuss a “variation” on MSE in equation
 250 (1) that bears some resemblance to my privacy deficit notion, defined as $h(x) = \max \{0, f_S(x) - f_D(x)\}$, in that it
 251 is asymmetric in penalization of under- and over-estimation of some quantity.

252 Minimizing MSE for estimates of a particular parameter θ is a fair goal for statistical analyses whose purpose
 253 is to conduct traditional hypothesis tests regarding the true value of θ in line with the Popperian falsification
 254 paradigm of science. Lower MSE generally would lead to higher statistical power and therefore greater ability to
 255 avoid Type II error in hypothesis tests. [Casella & Berger, 2002] write, “In general, the experimenter must consider
 256 the consequences of various errors in estimation for different values of θ and specify a loss function that reflects
 257 these consequences.” By minimizing bias and variance explicitly, MSE — as a loss function — performs well in
 258 avoiding the Type I and Type II error consequences in null hypothesis testing and therefore MSE often makes sense
 259 to use as a loss function in scientific hypothesis testing.

260 [Casella & Berger, 2002] go further and observe, “It would be an atypical decision theoretic analysis in which
 261 the set \mathcal{D} of allowable estimators was restricted to the set of unbiased estimators, as was done in Section 7.3.2.”
 262 As I highlighted, MLE typically has lowest variance, asymptotically, among estimators with zero bias. Therefore,
 263 restricting ourselves to MLE in tackling the problem before us — construction of the PDF for the decoy selection
 264 algorithm — would likely seem ill-advised to [Casella & Berger, 2002], since the class of unbiased estimators might
 265 not be suitable.

266 Note also that maximum likelihood estimators are point estimators for the particular θ parameters of PDFs. In
 267 theory, the estimated $\hat{\theta}$ will yield the corresponding theoretical distributions that fit the target empirical distributions
 268 well, although only under the assumption that the empirical distribution being fitted exactly equals the chosen
 269 theoretical PDF. There is no guarantee that variance — or bias for that matter — for the distribution itself will
 270 be small when using MLE to fit the wrong theoretical PDF to an empirical distribution. Given the fact that we
 271 are interested in the whole distributions themselves, i.e. $f_S(x)$ and $f_D(x)$, and not just parameters of parametric

273 distributions, the justification for using MLE in this setting is even weaker. In just a moment I will convert the
 274 problem of fitting distributions into a parametric one, so that the true problem is better illustrated.

275

276

277 Until now I have dealt with $f_S(x)$ and $f_D(x)$ as if they were probability density functions, i.e. as if the domain
 278 of the functions were continuous. However, in reality they are probability mass functions, i.e. the domain of the
 279 functions are discrete. The real spend age distributions are only meaningful in terms of the discrete blocks on the
 280 blockchain, since miners can arrange valid transactions within a block in any order they choose. We can leverage
 281 this fact for the following analysis.

282 Define a set of parameters θ as follows:

$$\theta = \{\theta_1, \theta_2, \dots, \theta_N\} = \{f_S(1), f_S(2), \dots, f_S(N)\}$$

283 So θ_1 is the value of $f_S(x)$ when $x = 1$, i.e. the first-available block that an output can be spent in. θ_N refers to
 284 the first block where RingCT outputs appeared. My definition here is not completely rigorous, since the blockchain
 285 is lengthening constantly, and therefore the number of elements of θ is increasing by the hour.

286 What we wish to estimate is θ — every element of it. Or, more specifically, we wish to construct some $f_D(x)$
 287 such that $f_D(x_i)$ is “close” — in some sense to be defined shortly — to each θ_i , for every i . With a nonparametric
 288 approach, we may be able to tackle each element θ_i individually, more or less. With a parametric approach, we
 289 cannot hope to do so. Therefore, we must establish some overall metric, or metrics, of “success”. In other words,
 290 we must define and justify a set \mathcal{L} of loss functions. This is our first task. Our second task is to define a set \mathcal{D} of
 291 allowable estimators.

292 In equation (2), [Casella & Berger, 2002] defined the risk function as $R(\theta, \delta) = E_\theta L(\theta, \delta(\mathbf{X}))$. For the time
 293 being, we will assume that θ is deterministic and therefore the risk function equals the loss function. The θ is
 294 actually stochastic — it changes over time as user spending patterns change over time — which will be dealt with
 295 in **Section 7 Dynamic Risk and Forecasting**.

296 There are some similarities between the Differential Privacy framework and Monero’s ring signature privacy
 297 model. Differential Privacy seeks a balance between the desire to perform statistical analysis on private data and
 298 the need to protect individuals from discovery of their private information. Monero seeks to maximize privacy
 299 of users, but is constrained by reasonable limits on ring size. I looked through the Differential Privacy literature
 300 for some criteria for fitting a decoy selection algorithm. In general there are utility-based criteria for resolving
 301 the balance between statistical analysis and user privacy for each user, but there is not yet a way to resolve our
 302 problem([Hsu et al., 2014]). Our problem is different in that a particular ring size is fixed, and then trade-offs
 303 between users need to be determined.

304 In “Research Roadmap for an Overhaul of Monero’s Mixin Selection Algorithm”, which I submitted to Monero’s
 305 Vulnerability Response Process in 2021, I wrote:

306 How do we construct $f_M(x)$ [the decoy selection algorithm] for best overall privacy if we restrict ourselves
 307 to parametric distributions, and therefore cannot achieve $f_S(x) \approx f_M(x)$ for all values of x ? Well, it
 308 depend [sic] on how we define “best”. Below are six approaches. I have the mathematical definitions of
 309 these worked out in my head, but they are not written here:

310

- 311 1) Privacy impoverishment
- 312 2) Economic welfare
- 313 3) Inequality minimization
- 314 4) Worst-case-scenario minimization
- 315 5) Maximum Likelihood Estimation

316 6) Maximize resistance to a specific attack

317

318 Now that a set of objective functions have been defined, one could imagine optimizing these objective
319 functions in a numerical optimization procedure where each parametric distribution family with support
320 of $[0, \infty)$ is permuted over 1-6 above.

321 These objective functions are the loss functions in the framework of [Casella & Berger, 2002]. Many of them are
322 forms of minimum divergence estimators ([Maji et al., 2019]). Just two more bits of housekeeping before I can
323 mathematically define these 1-6 loss functions. First, to be consistent with the notation of [Casella & Berger, 2002],
324 define $f_D(x_i) \equiv a_i$.

325 Second, we must think about how to give weight to each θ_i . Do we give equal weight to every θ_i ? That would
326 mean that outputs years old would be given the same importance as outputs just a few minutes or hours old.
327 Weighting the loss function by the value of θ_i seems more reasonable since that would, in effect, give each spent
328 output equal importance. However, we are trying to protect the privacy of people, not outputs.

329 Say that User A re-spends outputs frequently, and so has real spends that are in the thick portion of $f_S(x)$.
330 Say that User B re-spends outputs infrequently, and therefore has real spends that are in the thin portion of $f_S(x)$.
331 Furthermore, User A would be able to generate more transactions than User B simply because of rapidly re-spending
332 outputs. Therefore, only weighting the loss function by the value of θ_i would (maybe unfairly) give more importance
333 to User A than User B, just due to the way that the mathematics work out. The way forward is not exactly clear.
334 I think it could make sense to try several intermediate weighting schemes.

335 First, my recommendation is to only give weight to elements of $\boldsymbol{\theta}$ when there is a privacy deficit, i.e. when
336 $h(x) = \max \{0, f_S(x) - f_D(x)\}$ is nonzero. Later we will use $\mathbf{1}\{x\}$, the indicator function, for this part of the
337 weighting scheme, or the $\min \{x\}$ operator, depending on the context.³ For comparison purposes, I will also include
338 the symmetric counterpart $h_{sym}(x) = |f_S(x) - f_D(x)|$ that seeks to avoid privacy surpluses as much as it seeks to
339 avoid privacy deficits. To allow for multiple intermediate weighting schemes, define this weight function:

$$w(\theta_i, \lambda) = \lambda \theta_i + (1 - \lambda) \frac{1}{N} \quad (3)$$

340 Thus, when $\lambda = 1$, $w(\theta_i, \lambda)$ is fully weighted by the value of θ_i . When $\lambda = 0$, $w(\theta_i, \lambda)$ gives equal weight to each
341 θ_i . Tentatively, let $\boldsymbol{\lambda} = \{0, 0.5, 0.9, 0.95, 0.99, 0.999, 0.9999, 1\}$.

342 Now we are ready to define the set \mathcal{L} of loss functions.

343 4.1 Privacy impoverishment

344 To me, the privacy deficit formulation is somewhat reminiscent of a poverty line. Below a certain defined threshold
345 individuals are considered to be impoverished. In the case of a standard poverty indicator, there is some poverty
346 line z defined by a researcher or government entity. In the case of Monero user privacy, the corresponding “poverty
347 line” would be $f_S(x)$, which is different for every x .

348 The Foster–Greer–Thorbecke (FGT) indices are a family of widely-used poverty indicators. They are defined as

$$FGT_\alpha = \frac{1}{N} \sum_{i=1}^H \left(\frac{z - y_i}{z} \right)^\alpha$$

349 where N is the number of people in the population under study, H is the number of people within that population
350 who are below the poverty line, z is the poverty line, y_i is the income (or consumption) of each individual i who is
351 under the poverty line, and α is a parameter that controls weighting.

³https://en.wikipedia.org/wiki/Indicator_function

If α is high, then people far below the poverty line are given much more weight than people just barely below the poverty line. When $\alpha = 0$, FGT_0 is simply the poverty headcount. When $\alpha = 1$, FGT_1 is the poverty gap index. When $\alpha = 2$, FGT_2 weights each person's poverty gap by its square, and for $\alpha = 3$, by its cube, and so forth.

A loss function analogue can be defined:

$$L_{FGT_\alpha}(\boldsymbol{\theta}, \mathbf{a}, \lambda) = \frac{1}{N} \sum_{i=1}^N \mathbf{1}\{a_i < \theta_i\} w(\theta_i, \lambda) \left(\frac{\theta_i - a_i}{\theta_i} \right)^\alpha \quad (4)$$

The $\mathbf{1}\{a_i < \theta_i\}$ indicator function ensures that a_i 's are only counted when there is some privacy deficit. The symmetric counterpart $L_{FGT_{\alpha, sym}}(\boldsymbol{\theta}, \mathbf{a}, \lambda)$ would omit the $\mathbf{1}\{a_i < \theta_i\}$ term and replace $\left(\frac{\theta_i - a_i}{\theta_i} \right)^\alpha$ with $\left(\left| \frac{\theta_i - a_i}{\theta_i} \right| \right)^\alpha$. Using $\alpha = 0$ probably doesn't make sense for our purposes. Using $\alpha = \{1, 2, 3\}$ is reasonable.

4.2 Economic welfare

A full discussion of the meaning and theory of economic welfare is outside of the scope of this document. The basic idea is that people are theorized to have preferences that can be approximated via a mathematical function. These approximating functions are called utility functions. When people's preferences are satisfied, they obtain utility. When the preferences are satisfied to a higher degree, they obtain higher utility. In essence, when an individual's utility is higher, their happiness is higher. Within the framework of neoclassical economics, individuals strive to maximize their utility, subject to the constraints they encounter in the world. The analysis of aggregate population-level utility is the realm of welfare economics.

We may assume that Monero users prefer to have privacy and therefore some "privacy utility function" in this specific context could be defined. In practice, the loss function derived from this type of analysis will look similar to the $L_{FGT_\alpha}(\boldsymbol{\theta}, \mathbf{a}, \lambda)$ privacy impoverishment loss function, but with a different interpretation.

There are dozens of utility functions to choose from. One of the more appropriate ones in the present context is the Constant Relative Risk Aversion (CRRA) utility function:

$$u_{CRRA_\eta}(y) = \begin{cases} \frac{y^{1-\eta}}{1-\eta} & \eta \geq 0, \eta \neq 1 \\ \ln(y) & \eta = 1 \end{cases} \quad (5)$$

where η is the coefficient of constant relative risk aversion. The CRRA utility function makes sense to use in this context because (1) At a basic level, it takes a single argument, unlike other classes of utility functions that deal with multiple goods and services; (2) It explicitly deals with risk; (3) It has an adjustable parameter η that we can use to explore the sensitivity of the results; (4) For $\eta \geq 1$, the CRRA utility function approaches $-\infty$ as y approaches zero.

The (4) characteristic serves as an important advantage compared to the privacy impoverishment framework since in theory the $L_{FGT_\alpha}(\boldsymbol{\theta}, \mathbf{a}, \lambda)$ loss function would allow $f_D(x)$ to have zero mass at some x values — and therefore any ring members having an age corresponding to those x values would be clearly identifiable as real spends. In addition, a numerical optimization process that used the CRRA utility function as its basis would avoid at all costs $f_D(x) = 0$ for any and all x values as long as η is chosen so that $\eta \geq 1$.

In a welfare economics framework, generally some discussion of the Pareto weights and Pareto efficiency would be appropriate. However, that type of discussion has little practical effect on the analysis here and it would generally only be of interest to economists, so I will elide it here.

Now we are ready to define an economic welfare loss function:

$$L_{Welfare_\eta}(\boldsymbol{\theta}, \mathbf{a}, \lambda) = (-1) \frac{1}{N} \sum_{i=1}^N w(\theta_i, \lambda) \left(u_{CRRA_\eta} \left(\min \left\{ \frac{a_i}{\theta_i}, 1 \right\} \right) \right) \quad (6)$$

The (-1) scalar is to make this a *loss* function to be minimized. As is typical, the CRRA utility function increases with its argument, and privacy increases as a_i becomes closer to θ_i , i.e. as $f_D(i)$ becomes closer to $f_S(i)$. We use the $\min \{x\}$ operator here. When $a_i < \theta_i$, the utility function is applied to $\frac{a_i}{\theta_i}$. When $a_i \geq \theta_i$, the utility function is applied to one, as if $a_i = \theta_i$, since users spending outputs from this block i suffer no privacy deficit as I have defined it. The symmetric counterpart $L_{Welfare_{\eta,sym}}(\boldsymbol{\theta}, \mathbf{a}, \lambda)$ would replace $\min \left\{ \frac{a_i}{\theta_i}, 1 \right\}$ with $\frac{a_i}{\theta_i}$.

The choice for η is somewhat open-ended. Perhaps five values should be tested, to get some sense of the sensitivity of the results to the choice of η . One of the values should be $\eta = 1$ so that log utility is used. It is less clear what the remaining four values should be. Some experimentally-determined values for η for the utility of income are available in the literature, but how individuals' utility functions for income and privacy relate to one another is unclear. Tentatively, let us set $\boldsymbol{\eta}$ to $\boldsymbol{\eta} = \{0.5, 1, 2, 5\}$.

4.3 Inequality minimization

Another possible loss function is an inequality metric. The privacy impoverishment and economic welfare frameworks dealt with the absolute privacy of each user. We may also want to consider a framework that explicitly compares users to each other, in terms of the privacy that a $f_D(x)$ provides. A loss function that attempts to minimize inequality of privacy among users may be appropriate.

One of the most widely-used inequality metrics is the Gini coefficient (or Gini index). The Gini coefficient has many attractive theoretical properties that I will not recite here. Its main drawback is that its value is not very interpretable for laypeople. (The most intuitive explanation involves the Lorenz curve.) Given that we are already far into the realm of difficulty with interpretation of these loss functions, the low interpretability of the Gini coefficient should not stop us from using it.

One formulation of the Gini coefficient is:

$$G(\mathbf{x}) = \frac{\sum_{i=1}^n \sum_{j=1}^n |x_i - x_j|}{2 \sum_{i=1}^n \sum_{j=1}^n x_j} = \frac{\sum_{i=1}^n \sum_{j=1}^n |x_i - x_j|}{2n^2 \bar{x}}$$

This formulation is somewhat easy to interpret, although it is computationally expensive as it requires about $(n^2 - n)/2$ arithmetic operations. It does not contemplate weights, so it must be modified. [Creedy, 2015] provides some guidance.

First, the formula suggested by Creedy requires that the weights sum up to n , i.e. $\sum_{i=1}^n w_i = n$. The weights that we will use, $w(\theta_i, \lambda)$ could easily be normalized to ensure $\sum_{i=1}^n w(\theta_i, \lambda) = n$.

In his equation (17), Creedy suggests the following weighted formula:

$$G(\mathbf{x}) = \frac{\sum_{i=1}^n \sum_{j=i+1}^n w_i w_j |x_i - x_j|}{\sum_{i=1}^n w_i \sum_{i=1}^n w_i x_i}$$

If we let x_i be $\frac{a_i}{\theta_i}$ as with the economic welfare loss function, the corresponding loss function for our problem would then be:

$$L_{Gini}(\boldsymbol{\theta}, \mathbf{a}, \lambda) = \frac{\sum_{i=1}^n \sum_{j=i+1}^n w(\theta_i, \lambda) \cdot w(\theta_j, a_j, \lambda) \cdot \left| \min \left\{ \frac{a_i}{\theta_i}, 1 \right\} - \min \left\{ \frac{a_j}{\theta_j}, 1 \right\} \right|}{\sum_{i=1}^n w(\theta_i, \lambda) \sum_{i=1}^n w(\theta_i, \lambda) \cdot \min \left\{ \frac{a_i}{\theta_i}, 1 \right\}} \quad (7)$$

subject to $\sum_{i=1}^n w(\theta_i, \lambda) = n$

416 Note that the formula given in equation (17) in [Creedy, 2015] is just one possible way to deal with weighting
417 to compute a Gini coefficient. The reason that there are multiple ways to do weighting is that weighting attempts
418 to, in essence, interpolate parts of the Lorenz curve. How to do that interpolation is up for debate. In his equation
419 (12), [Creedy, 2015] also gives a weighted Gini formula that is less computationally expensive. However, it would
420 require conversion of $w(\theta_i, \lambda)$ to integers, which is feasible but adds another layer of complication. The symmetric
421 counterpart $L_{Gini,sym}(\boldsymbol{\theta}, \mathbf{a}, \lambda)$ would replace $\min \left\{ \frac{a_i}{\theta_i}, 1 \right\}$ with $\frac{a_i}{\theta_i}$.

422 4.4 Worst-case-scenario minimization

423 Worst-case-scenario minimization is inspired by Appendix F: Minimum Untraceability in [Möser et al., 2018]. They
424 define Ge_{min} , the minimum possible guessing entropy of the untraceability of a transaction input:

$$Ge_{min} = \frac{\frac{1}{2}m(m+1)}{\frac{r_{max}}{r_{min}} + m} \quad (8)$$

425 where m is the number of ring members and

$$r_{max} = \max_{\forall x} \left(\frac{f_S(x)}{f_D(x)} \right), r_{min} = \min_{\forall x} \left(\frac{f_S(x)}{f_D(x)} \right)$$

426 Since m is a constant, and optimization procedures are insensitive to constants, for the purposes of constructing
427 a loss function, Ge_{min} can be simplified to

$$Ge_{min(optimizer)} = \frac{r_{max}}{r_{min}} \quad (9)$$

428 The logic to construct $Ge_{min(optimizer)}$ is as follows:

$$\begin{aligned} Ge_{min(optimizer)} &= \frac{\frac{1}{2}m(m+1)}{\frac{r_{max}}{r_{min}} + m} \\ &\propto \frac{1}{\frac{r_{max}}{r_{min}} + m} && \text{scaling by } \left(\frac{1}{2}m(m+1) \right)^{-1} \text{ is a monotonic transformation} \\ &\cong \frac{r_{max}}{r_{min}} + m && g(x) = \frac{1}{x} \text{ is a strictly decreasing monotonic transformation} \\ &\cong \frac{r_{max}}{r_{min}} && \text{subtracting } m \text{ is a monotonic transformation} \end{aligned}$$

429 (I am using the \cong symbol loosely here.) Therefore, a $f_D(x)$ that minimizes (9) will also maximize (8)

430

431 Putting these ideas into the loss function notation that I have been using, i.e.

$$r_{max} = \max_{\forall i} \left(\frac{\theta_i}{a_i} \right), r_{min} = \min_{\forall i} \left(\frac{\theta_i}{a_i} \right)$$

432 gives us

$$L_{Worst\ case}(\boldsymbol{\theta}, \mathbf{a}) = \frac{\max_{i \in \{1, \dots, N\}} \left(\frac{\theta_i}{a_i} \right)}{\min_{i \in \{1, \dots, N\}} \left(\frac{\theta_i}{a_i} \right)} \quad (10)$$

433 It is not clear to me how weighting by $w(\theta_i, \lambda)$ might work here since the numerator and denominator are both
434 single numbers. For the time being I will leave it out.

435 Although I include $L_{Worst\ case}$ in the proposed set \mathcal{L} of loss functions, I am skeptical of its usefulness. It is
436 not clear to me that we should care about the minimum θ_i and a_i among literally hundreds of thousands of them.
437 Maybe the tail should not wag the dog. However, it could serve as a useful comparison to other approaches, so I
438 include it in \mathcal{L} . Another issue is that I suspect that $L_{Worst\ case}$ will not be a well-behaved function for the purposes
439 of numerical optimization. Given the min and max operators and how they are used here, I foresee that $L_{Worst\ case}$
440 as a function will have some significant discontinuities with respect to i .

441 4.5 Maximum Likelihood Estimation

442 As I have stated, I do not favor a MLE approach here. However, including it in the set of loss functions \mathcal{L} might
443 serve as a useful comparison.

444 Let $\boldsymbol{\beta} = \{\beta_1, \dots, \beta_k\}$ be the set of parameters of some parametric probability density function $g(x|\boldsymbol{\beta})$. Then the
445 likelihood function for some sample \mathbf{x} is

$$L(\boldsymbol{\beta}|\mathbf{x}) = \prod_{i=1}^n g(x_i|\boldsymbol{\beta})$$

446 To put MLE in a loss function framework, convert it into a minimization problem and take the log to ease the
447 computational burden:

$$L_{MLE}(\boldsymbol{\beta}|\mathbf{x}) = (-1) \cdot \sum_{i=1}^n \log g(x_i|\boldsymbol{\beta}) \quad (11)$$

448 4.6 Maximize Resistance to an Attack

449 Define the potency of an attack on the untraceability of Monero transactions for a specified $f_D(x)$ as $\mathcal{P}(f_D(x))$,
450 the unconditional probability of correctly guessing the real spend. Then the corresponding loss function can be
451 defined as

$$L_{Attack}(f_D(x)) = \mathcal{P}(f_D(x)) \quad (12)$$

452

453

454 Now that the set \mathcal{L} of loss functions has been defined, the set \mathcal{D} of allowable estimators will be defined. Continuing
455 with the θ_i notation, the allowable estimators will be selected from the set of parametric probability density functions
456 (PDF) $f(x|\boldsymbol{\beta})$ such that each θ_i shall be estimated by the image of i under $f(x|\boldsymbol{\beta})$. In other words, $\hat{\theta}_i = f(i|\boldsymbol{\beta})$
457 for all i .

458 Strictly speaking, the estimator here is the minimizer of a specified loss function in the set \mathcal{L} where $a_i = f(i)$
459 for all i for some specified parametric PDF $f(x|\boldsymbol{\beta})$. The set of all PDFs (and probability mass functions (PMFs),
460 for that matter) can be all PDFs whose support is the set $[0, \infty)$. The Wikipedia page on probability distributions

⁴⁶¹ lists over 40 distributions that have such a support.⁴ So let us say that the target number of elements of the set
⁴⁶² of PDFs used in estimation is 40. Note that many distributions are special cases of more general distributions and
⁴⁶³ therefore the actual number of distributions to fit may be lower than 40 in practice. Define the set \mathcal{F} of these PDFs.
⁴⁶⁴ Let \mathcal{B} be the set of parameters of each $f(x|\beta)$ under consideration.

⁴⁶⁵ 4.7 Formalized Optimization Criteria

⁴⁶⁶ First, assume we have a good estimate of $f_S(x)$. Then OSPEAD is the set of procedures that perform the following
⁴⁶⁷ minimizations:

$\forall L \in \mathcal{L},$	Loss functions
$\forall f(x \beta) \in \mathcal{F},$	Parametric distributions
$\forall \lambda \in \boldsymbol{\lambda},$	Weight parameters for $w(\theta_i, \lambda)$
$\forall \alpha \in \boldsymbol{\alpha},$	Exponents for FGT poverty indicator
$\forall \eta \in \boldsymbol{\eta},$	Parameters for CRRA utility
$\min_{\beta \in \mathcal{B}} L(f(x \beta))$	Numerical optimization problems

⁽¹³⁾

where

$$\mathcal{L} = \{L_{FGT_\alpha}, L_{Welfare_\eta}, L_{Gini}, L_{Worst\ case}, L_{MLE}, L_{Attack}\} \quad \text{Equations (4), (6), (7), (10), (11), (12)}$$

$$\mathcal{F} = \{\text{Roughly 40 PDF/PMFs that have support } [0, \infty)\}$$

$$\boldsymbol{\lambda} = \{0, 0.5, 0.9, 0.95, 0.99, 0.999, 0.9999, 1\}$$

$$\boldsymbol{\alpha} = \{1, 2, 3\}$$

$$\boldsymbol{\eta} = \{0.5, 1, 5, 10, 50\}$$

$$\mathcal{B} = \{\text{Sets of parameters associated with each element of } \mathcal{F}\}$$

⁴⁶⁸ For each loss function there will likely be a unique minimizer $f^*(x|\beta)$. However, it is unlikely that every loss
⁴⁶⁹ function will have the same minimizer. Therefore, determining which candidate $f(x|\beta)$ is “best” will be the result
⁴⁷⁰ of a judgment call, taking into account the totality of evidence and theory.

⁴⁷¹ Why stop with single PDFs when we could also examine mixture distributions? It would be useful to test some
⁴⁷² mixture distributions composed of two or three different parametric PDFs. The main difficulty is the combinatorics:
⁴⁷³ The number of two-PDF mixture distributions would be $\binom{40}{2} = 780$. Given the loss functions and their variations,
⁴⁷⁴ that would amount to about 58,500 numerical minimization procedures. There are already practical difficulties
⁴⁷⁵ with carrying out the minimizations with no mixture distributions. Starting values have to be defined and robust
⁴⁷⁶ minimization algorithms must be chosen and checked for problems. Even with no mixture distributions, the number
⁴⁷⁷ of minimizations that I set out to perform, as stated in (13), is about 3,000.⁵

⁴⁷⁸ Therefore, it could make sense to choose a small set of the most promising or complementary PDFs to do a
⁴⁷⁹ second round of OSPEAD with mixture distributions. Another possible enhancement could be incorporating some
⁴⁸⁰ periodic component in a mixture distribution to account for users’ sleep-wake cycle.

⁴[https://en.wikipedia.org/wiki/List_of_probability_distributions#Supported_on_semi-infinite_intervals,_usually_\[0,%E2%88%9E](https://en.wikipedia.org/wiki/List_of_probability_distributions#Supported_on_semi-infinite_intervals,_usually_[0,%E2%88%9E)

⁵Let $|\mathbf{S}|$ denote the cardinality of set \mathbf{S} . Note that $|\boldsymbol{\lambda}| = 8$, $|\boldsymbol{\alpha}| = 3$, $|\boldsymbol{\eta}| = 5$, and $|\mathcal{F}| = 40$. Taking into account the different flavors of the loss functions, $|L_{FGT_\alpha}(\theta, \mathbf{a}, \lambda)| = |\boldsymbol{\lambda}| \cdot |\boldsymbol{\alpha}| = 24$, $|L_{Welfare_\eta}(\theta, \mathbf{a}, \lambda)| = |\boldsymbol{\lambda}| \cdot |\boldsymbol{\eta}| = 40$, $|L_{Gini}(\theta, \mathbf{a}, \lambda)| = |\boldsymbol{\lambda}| = 8$, $|L_{Worst\ case}(\theta, \mathbf{a})| = 1$, $|L_{MLE}(\beta|\mathbf{x})| = 1$, and $|L_{RRRA}(f_D(x))| = 1$. Therefore, $|\mathcal{L}| = 75$ and hence $|\mathcal{L}| \cdot |\mathcal{F}| = 3,000$.

5 Dry Run with Old Möser et al. (2018) Data

To see how the minimizers in (13) would work in practice, we can perform a dry run on partially de-anonymized Monero spend age data provided by [Möser et al., 2018] from before February 2017. The final version of OSPEAD will use data from about September 2021 to October 2022, but the dry run is useful as a demonstration.

In the dry run I use a subset of the loss function and distribution functions described in (13). For the loss functions I select L_{FGT_α} with $\alpha = \{1, 2\}$, $L_{Welfare_\eta}$ with $\eta = \{0.5, 1\}$, and L_{MLE} . For the distribution function I choose the Log-gamma, Noncentral F, Right-Pareto Log-normal, Generalized Extreme Value, and Generalized Hyperbolic distributions. I also include mixtures of Log-gamma with F, Generalized Extreme Value, and a Laplace Periodic distribution.

Log-gamma: A two-parameter distribution used to fit the spend age data in [Möser et al., 2018]. The current decoy selection algorithm is based on a particular form of the Log-gamma distribution. The Gamma distribution includes the exponential, Erlang, and chi-square distributions as special cases.

Noncentral F: A three-parameter distribution used often in hypothesis testing.

Right-Pareto Log-normal: A three-parameter distribution that is a special case of the Double Pareto-lognormal distribution, which “arises as that of the state of a geometric Brownian motion (GBM), with lognormally distributed initial state, after an exponentially distributed length of time” [Reed & Jorgensen, 2004].

Generalized Extreme Value: A three-parameter distribution that includes the Gumbel, Fréchet and Weibull distributions as special cases.

Generalized Hyperbolic A six-parameter distribution that includes the Normal Inverse Gaussian, Variance Gamma, and Generalized Hyperbolic Student-t distributions as special cases.

Table 2: Performance of Dry Run with Old Möser et al. (2018) Data

Loss function	L_FGT	L_FGT	L_Welfare	L_Welfare	L_MLE
Loss function parameter	1	2	0.5	1	
Log-gamma	0.1138	0.0574	-1.8542	0.1955	7.65e+07
F	0.1095	0.0462	-1.8681	0.1635	7.67e+07
Right-Pareto Log-normal	0.1073	0.0449	-1.8703	0.1604	7.66e+07
Generalized Extreme Value	0.1169	0.0503	-1.8608	0.1766	7.76e+07
Generalized Hyperbolic	0.1100	0.0455	-1.8684	0.1632	7.62e+07
Log-gamma + F mix	0.1081	0.0402	-1.8721	0.1622	
Log-gamma + GEV mix	0.1095	0.0460	-1.8704	0.1547	
Log-gamma + Laplace Periodic	0.112	0.0572	-1.86	0.195	

Note: Values should be compared down columns. Lower values (darker green) indicate better performance. MLE value is Akaike Information Criterion (AIC).

Table 2 contains the values of the minimums for the various loss functions and parametric distributions. These numbers are useful for demonstration purposes, but the final numbers will look very different. We can see that

the Log-gamma distribution tends to compare poorly to the other distributions. The Right-Pareto Log-normal distribution tends to perform better than other pure distributions. The Log-gamma has poor performance and the F has mediocre performance, but when they are combined in a mixture distribution their performance is consistently good.

Table 3 contains the optimized parameter values for the various loss functions and parametric distributions. An important fact to recognize is that a particular set of parameter values that gives good performance according to one loss function may give poor performance for a different loss function. In these exercises we are not comparing a fixed set of parameter values across various loss functions. Rather, we are allowing each distribution's parameters to be bent to minimize each loss function value.

Following Table 3 is a series of plots showing the fitted distributions. The vertical black lines represent the empirical probability mass function. The vertical green lines extending below the horizontal axis represents the empirical cumulative distribution function. 76 percent of the mass of the Möser et al. (2018) data is less than 10,000 blocks old.

The first five plots show the fitted PDFs themselves. To compare the fitted distribution more closely with the empirical data, the second set of five plots shows the ratio of the fitted distributions $f_D(x)$ to the empirical probability mass function $f_S(x)$.

The code for producing these tables and plots is at <https://github.com/Rucknium/OSPEAD>

Table 3: Optimized Parameter Values of Dry Run with Old Möser et al. (2018) Data

Distribution	Loss fn	Loss fn param	param_1	param_2	param_3
F	L_FGT	1	0.0258	0.471	7.26
F	L_FGT	2	0.0338	0.294	10.3
F	L_Welfare	0.5	0.0289	0.429	8.1
F	L_Welfare	1	0.0333	0.383	9.27
F	L_MLE	0	0.0473	0.685	11.5
Generalized Extreme Value	L_FGT	1	106	421	2.63
Generalized Extreme Value	L_FGT	2	-72.7	3.14e-29	5.74
Generalized Extreme Value	L_Welfare	0.5	-95.9	1.92e-18	3.88
Generalized Extreme Value	L_Welfare	1	-86.6	6.28e-15	4.34
Generalized Extreme Value	L_MLE	0	99.7	246	2.48
Log-gamma	L_FGT	1	6.48	0.894	
Log-gamma	L_FGT	2	5.15	0.639	
Log-gamma	L_Welfare	0.5	6.25	0.852	
Log-gamma	L_Welfare	1	5.79	0.76	
Log-gamma	L_MLE	0	6.62	0.912	
Right-Pareto Log-normal	L_FGT	1	0.235	4.12	1.38
Right-Pareto Log-normal	L_FGT	2	0.133	3.79	1.21
Right-Pareto Log-normal	L_Welfare	0.5	0.209	4.03	1.32
Right-Pareto Log-normal	L_Welfare	1	0.18	3.92	1.25
Right-Pareto Log-normal	L_MLE	0	0.444	4.99	1.83

F Distribution: param_1 is first degree of freedom parameter; param_2 is second degree of freedom parameter; param_3 is non-centrality parameter.

Generalized Extreme Value Distribution: param_1 is location parameter; param_2 is scale parameter; param_3 is shape parameter.

Log-gamma Distribution: param_1 is shape parameter; param_2 is rate parameter.

Right-Pareto Log-normal Distribution: param_1 is shape parameter; param_2 is mean parameter; param_3 is variance parameter.

Mixture distributions and Generalized Hyperbolic Distribution are omitted from this table.

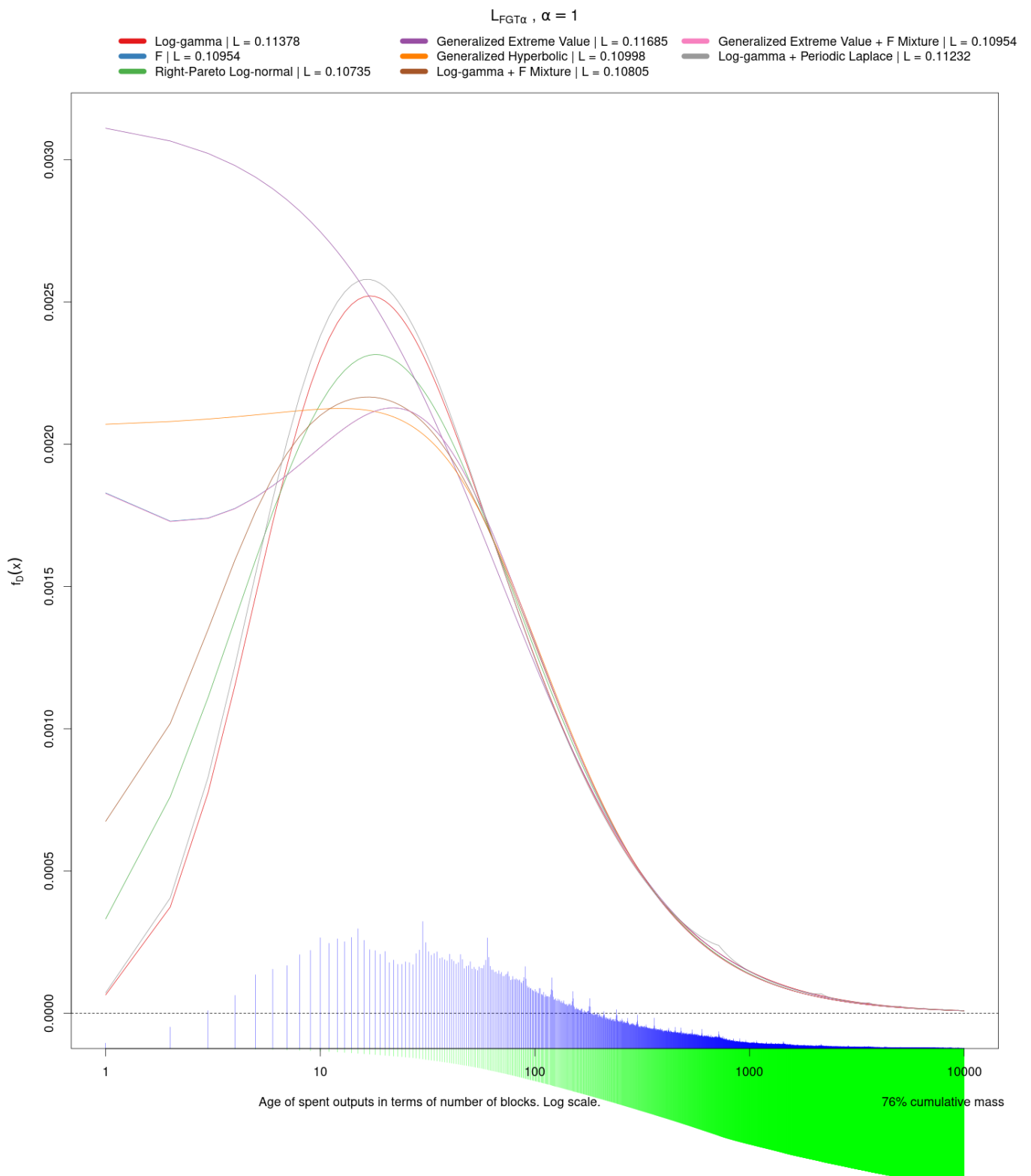
Figure 3: Optimized $f_D(x)$ for loss function L_{FGT_α} , $\alpha = 1$ 

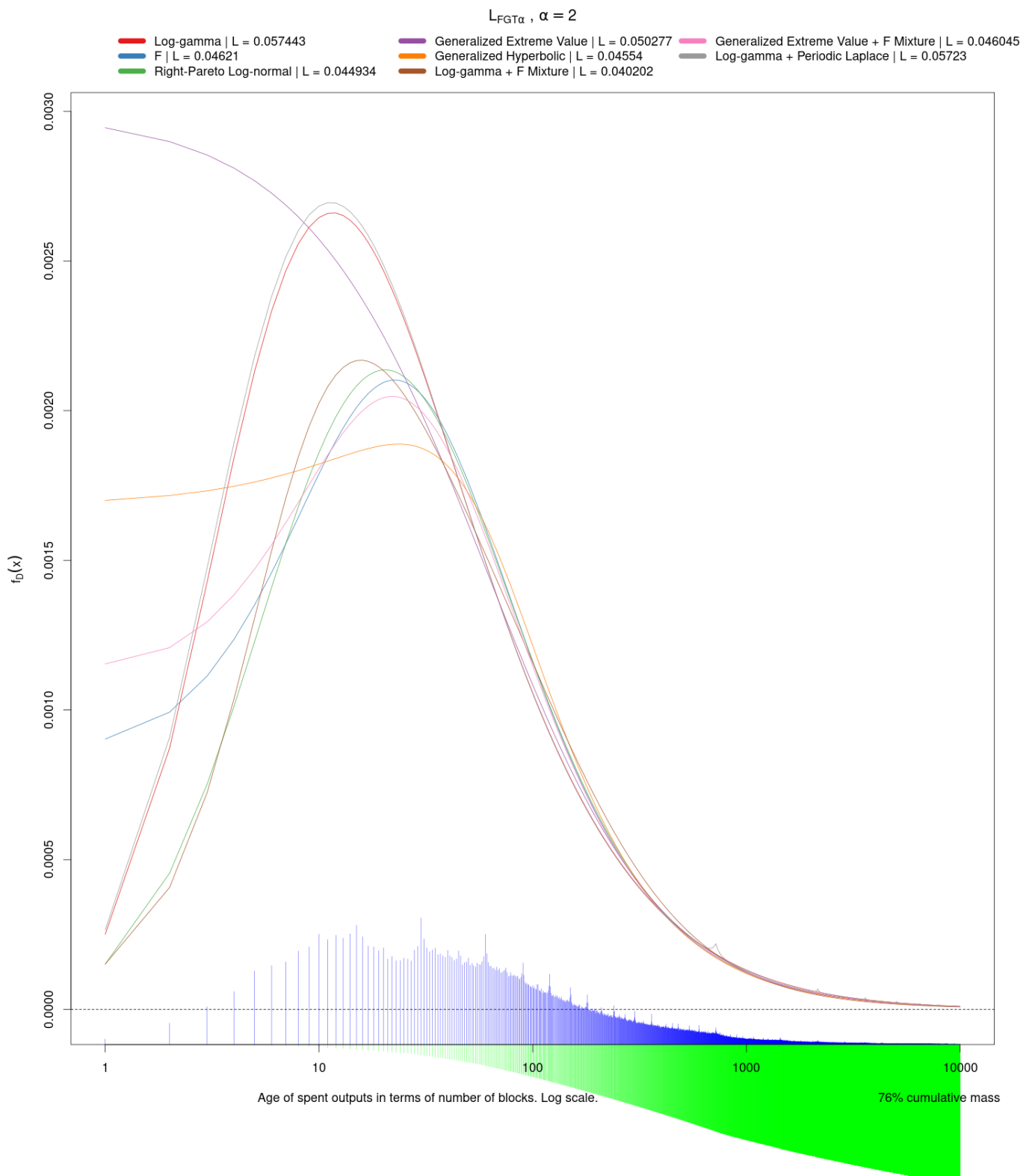
Figure 4: Optimized $f_D(x)$ for loss function L_{FGT_α} , $\alpha = 2$ 

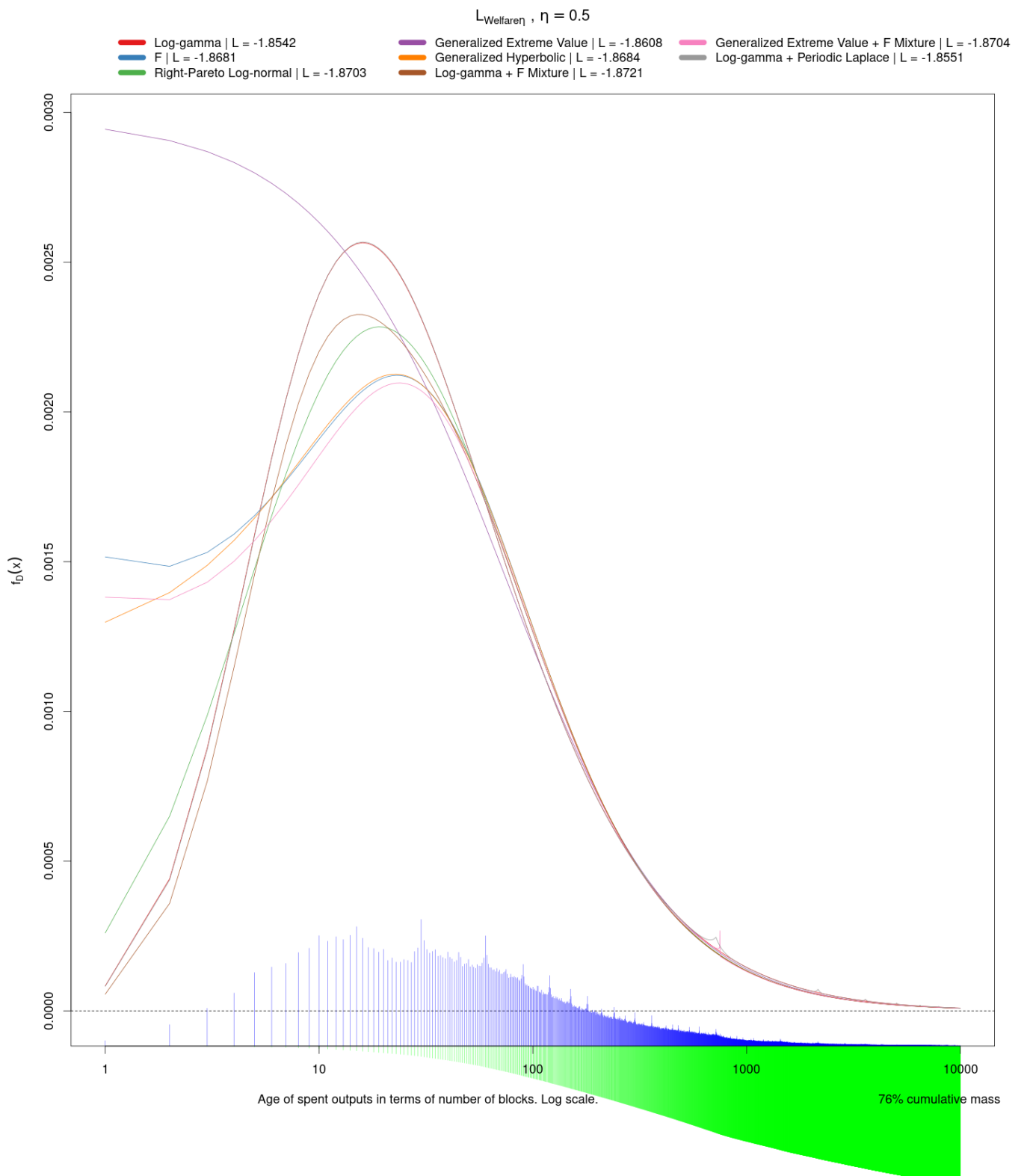
Figure 5: Optimized $f_D(x)$ for loss function $L_{Welfare_\eta}$, $\eta = 0.5$ 

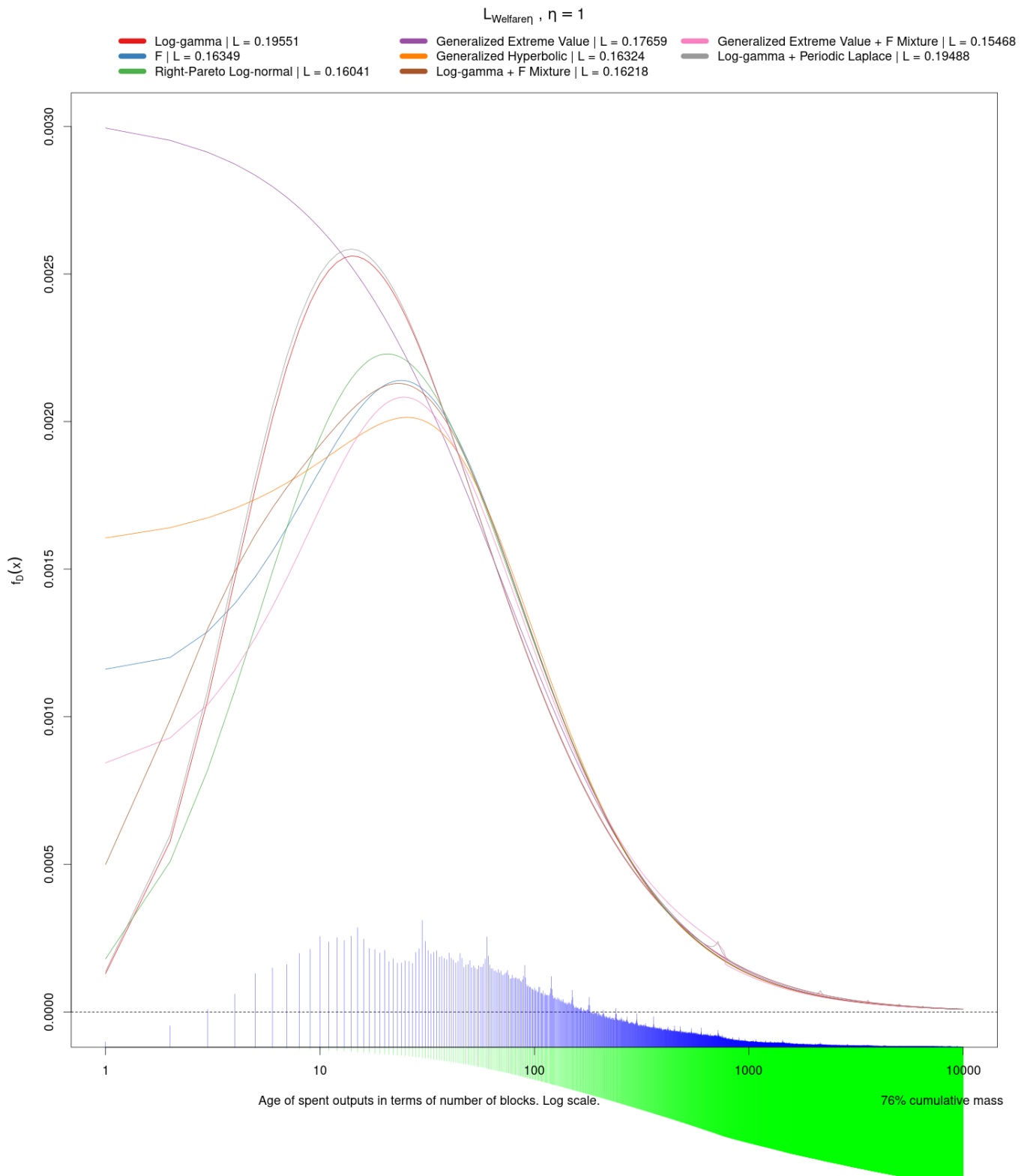
Figure 6: Optimized $f_D(x)$ for loss function $L_{Welfare_\eta}$, $\eta = 1$ 

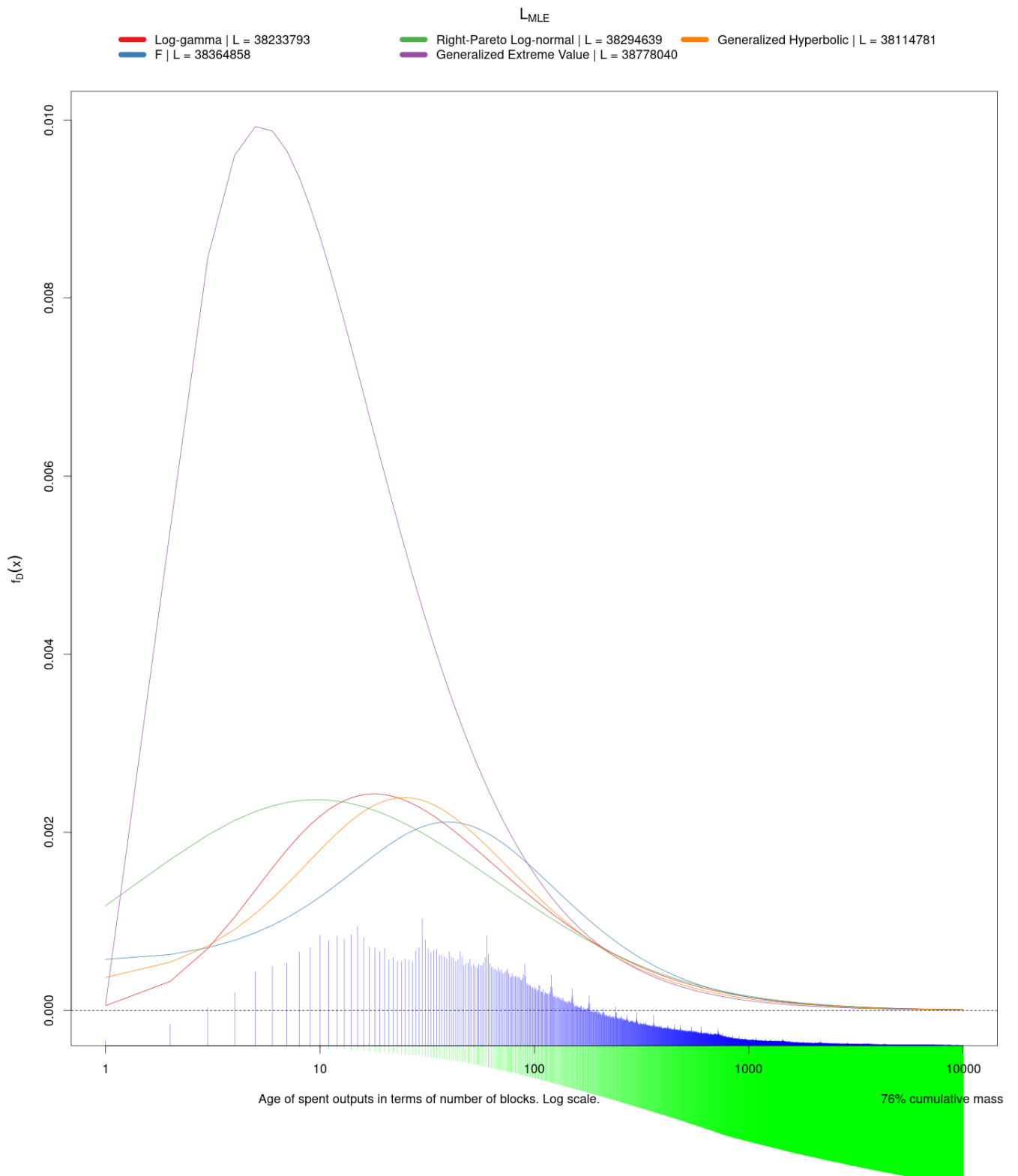
Figure 7: Optimized $f_D(x)$ for loss function L_{MLE} 

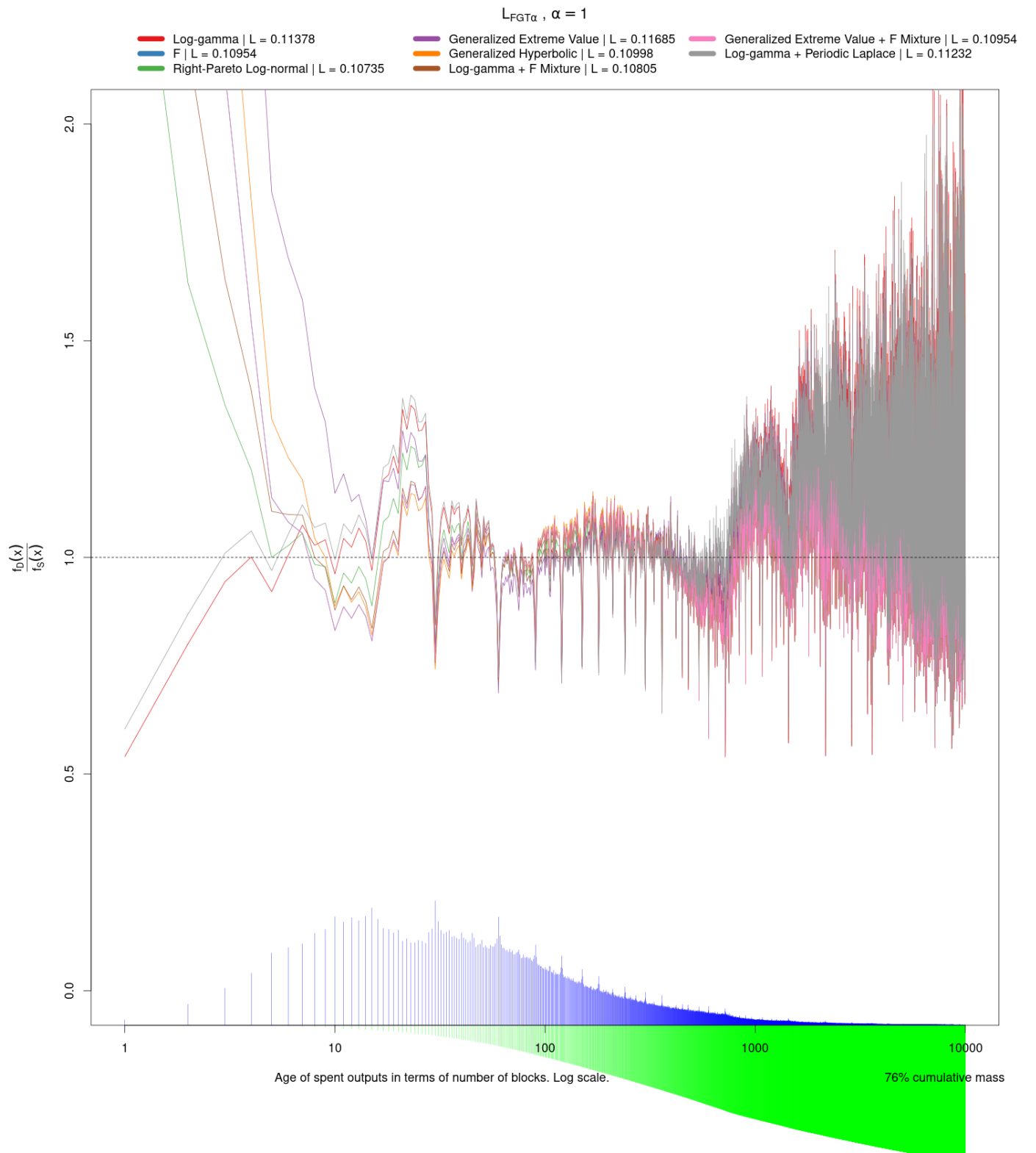
Figure 8: Optimized $f_D(x)/f_S(x)$ for loss function L_{FGT_α} , $\alpha = 1$ 

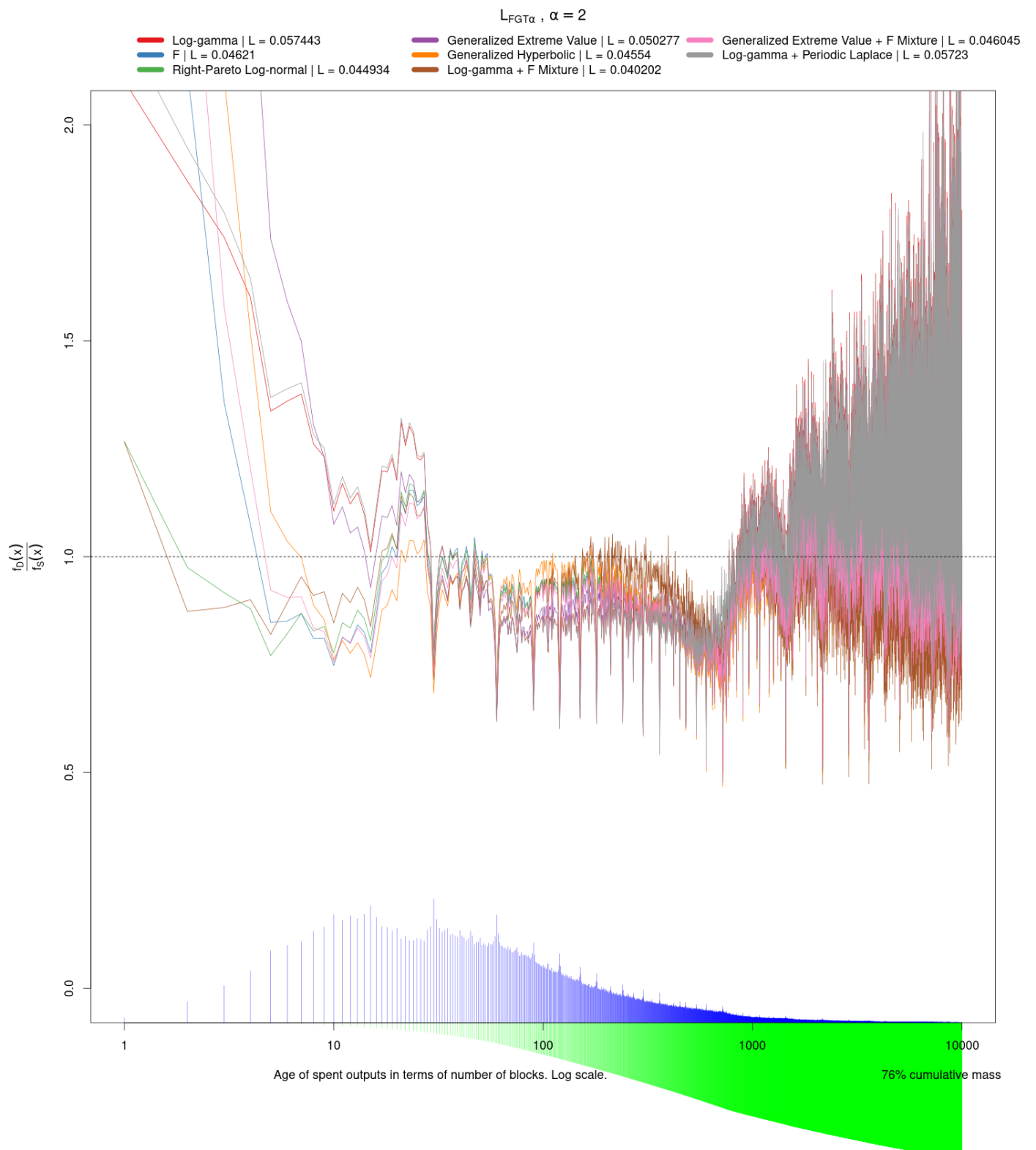
Figure 9: Optimized $f_D(x)/f_S(x)$ for loss function L_{FGT_α} , $\alpha = 2$ 

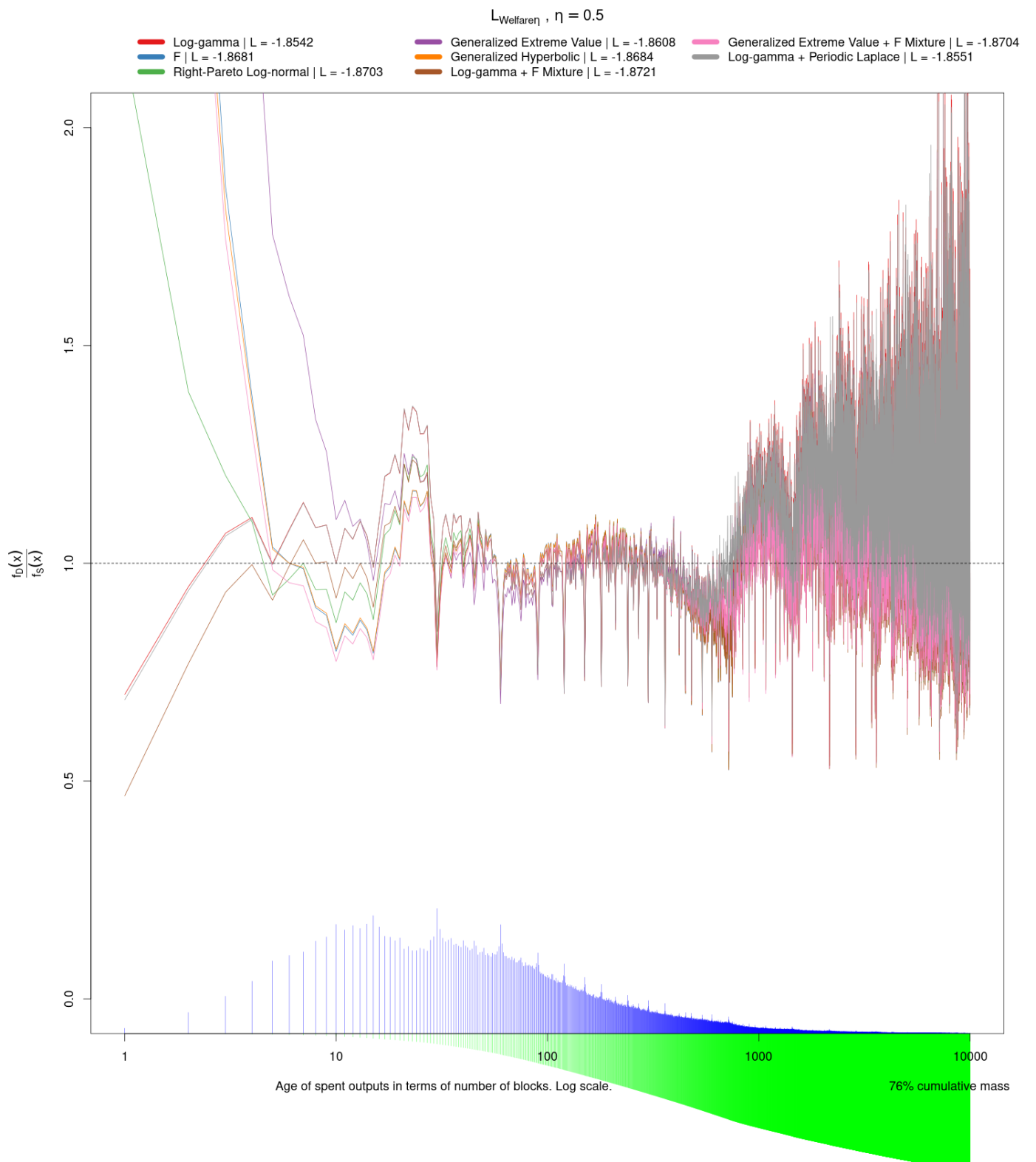
Figure 10: Optimized $f_D(x)/f_S(x)$ for loss function $L_{Welfare_\eta}$, $\eta = 0.5$ 

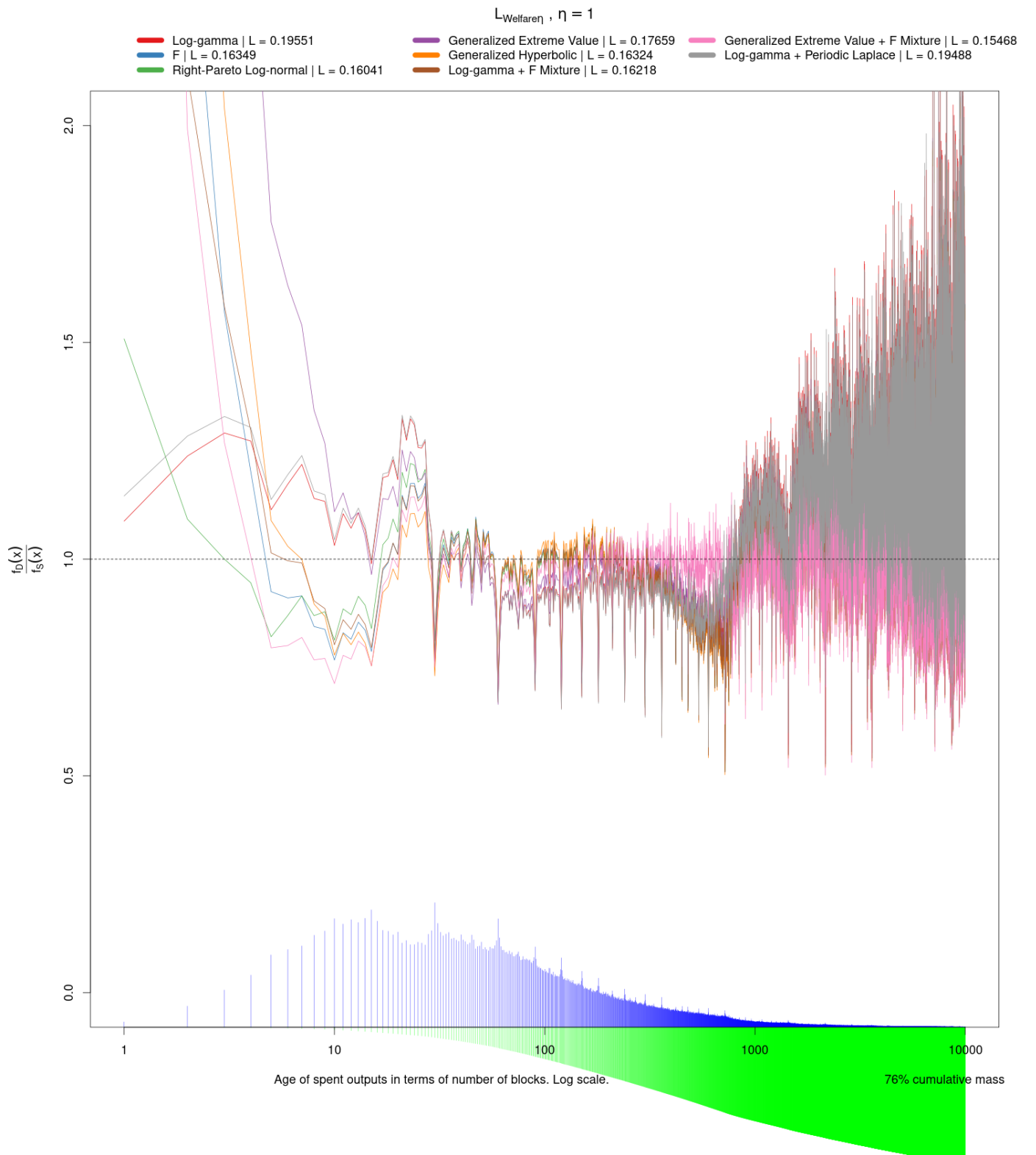
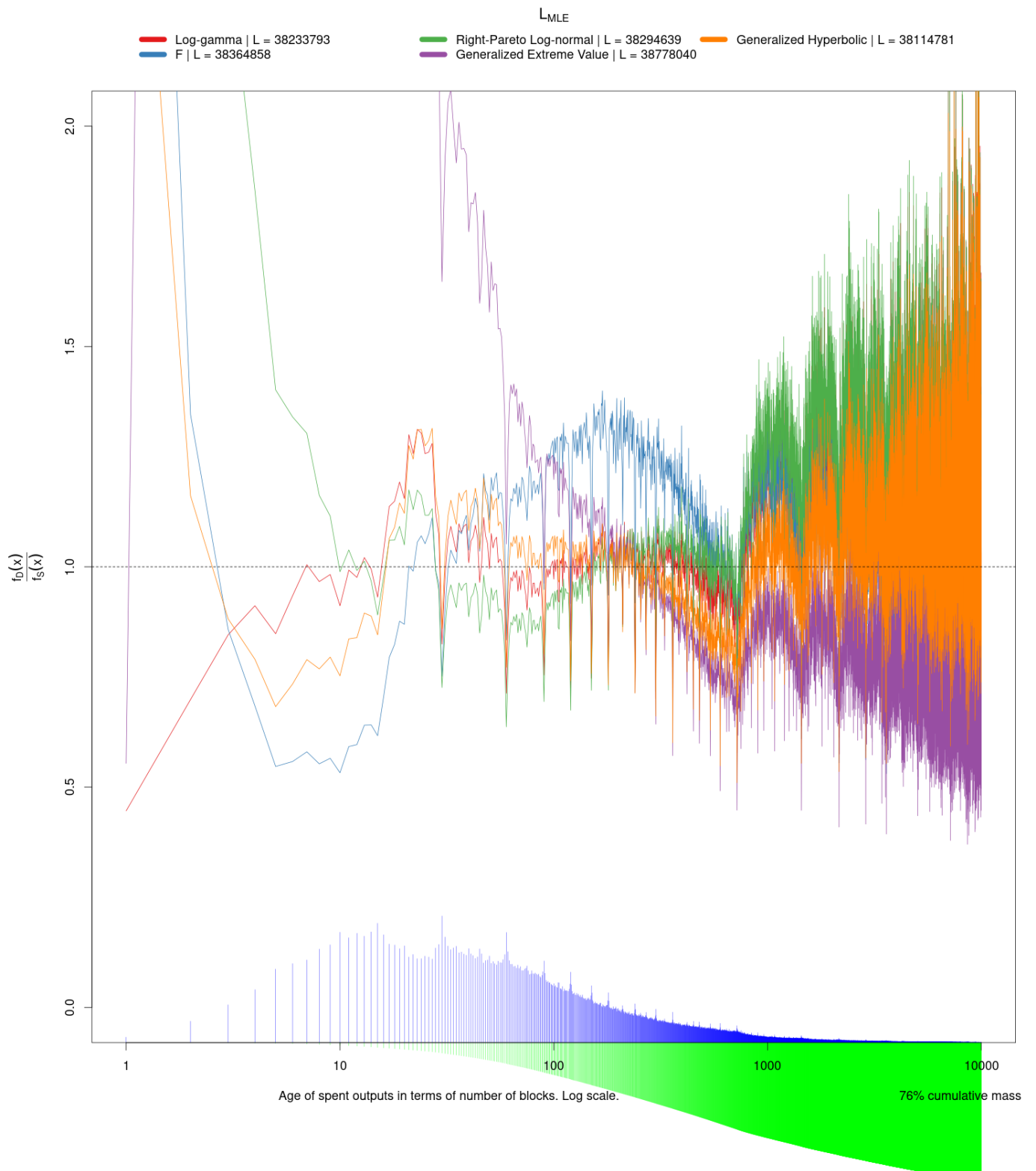
Figure 11: Optimized $f_D(x)/f_S(x)$ for loss function $L_{Welfare_\eta}$, $\eta = 1$ 

Figure 12: Optimized $f_D(x)/f_S(x)$ for loss function L_{MLE} 

6 Options for Loss Functions \mathcal{L} and Parametric Distributions \mathcal{F}

In Section 4 Criteria for Best Fit I developed several loss functions that could be used to decide which parametric distribution (and particular parameter values) should be used to form the OSPEAD decoy selection algorithm. At this point in time, it is not necessary to decide which loss function to use. We can perform the minimizations, examine the results, and make a decision when we have all the information.

1. Privacy impoverishment. This loss function overall appears to be one of the better choices. It is intuitive and provides options in its α parameter. To minimize risk of very low coverage of certain intervals on the probability distribution, setting $\alpha \geq 2$ would probably be best.
 2. Economic welfare. This criteria is less intuitive than privacy impoverishment, but it offers another way to adjust the risk sensitivity with its η parameter. Setting $\eta \geq 1$ will force more risk avoidance.
 3. Inequality minimization. This criteria would be most important if we seek to minimize inequality among users. One of its main drawbacks is that is can be computationally expensive.
 4. Worst-case-scenario minimization. This criteria has some appeal because worst case scenarios seem to be a focus in the field of cryptography. However, focusing on the worst case out of hundreds of thousands may be questionable.
 5. Maximum Likelihood Estimation. [Möser et al., 2018] used this criteria. For reasons stated above, I do not recommend this one.
 6. Maximize resistance to a specific attack. This criteria has some intuitive appeal: defend against an attack directly. However, it is difficult to say whether maximizing resistance to one attack may leave users vulnerable to a different attack.
- There is no particular statistical theoretical reason to choose one parametric distribution over another. Issues with software implementation may push us to use a simpler and more common distribution. If wallet developers do not use the `wallet2` implementation, they may have difficulty implementing a distribution defined by a mixture of unusual distributions.

544 7 Dynamic Risk and Forecasting

545 The Monero Research Lab research bulletin that I quoted in the introduction continues with the following observa-
 546 tion [Mackenzie et al., 2015]:

547 This would suggest that we, the developers of Monero, must estimate the probability distribution gov-
 548 erning the age of transaction outputs.

549 This, too, is problematic. When an exchange rate is experiencing a strong long-term decline (inflation),
 550 rational users are more likely to spend their transaction outputs, for tomorrow their outputs will be
 551 worth less in terms of goods and services than today and hoarding is not economically rational. When
 552 an exchange rate is experiencing a strong long-term increase (deflation), rational users are more likely to
 553 hoard their transaction outputs for the opposite reason. Hence, the distribution of transaction output
 554 ages will at least vary over time, and, presuming any proportion of users are rational will certainly depend
 555 sensitively on the economic performance of the currency. It is unwise to design security recommendations
 556 around the economic performance of our protocol.

557 I would argue that, as long as Monero is committed to using a mimicking decoy selection algorithm, “design[ing]
 558 security recommendations around the economic performance of our protocol” is unavoidable, if unfortunate. The
 559 best that we can do is to minimize the risk of guessing the future distribution incorrectly. This requires an assessment
 560 of dynamic risk with forecasting. According to empirical evidence from transparent chains, the spent output
 561 age distribution is affected more by volatility than long-term inflation and deflation. [Makarov & Schoar, 2021]
 562 concluded that “the vast majority of Bitcoin transactions between real entities are for trading and speculative
 563 purposes. Starting from 2015, 75% of real bitcoin volume has been linked to exchanges or exchange-like entities
 564 such as on-line wallets, OTC desks, and large institutional traders.” I discussed my own findings for DOGE in the
 565 June 1, 2022 Monero Research Lab meeting.⁶ The transaction patterns of Monero may be somewhat different due
 566 to its absence from many centralized exchanges, but probably not completely different. Assume for a moment that
 567 changes in the real spend age distribution are entirely caused by exchange rate volatility. In that case, forecasting
 568 the real spend age distribution would be roughly equivalent to forecasting exchange rate volatility and therefore
 569 would be highly challenging. The Efficient Market Hypothesis would imply that a naive forecast may be the best
 570 forecast.

571 We return to Equation (2) from **Section 4 Criteria for Best Fit**: the risk function $R(\theta, \delta) = E_\theta L(\theta, \delta(\mathbf{X}))$.
 572 This is the expected value of our choice of the loss function when a particular set of parameters, e.g. the shape,
 573 scale, and location of a parametric distribution, are set to particular values. The theoretical bounds on $R(\theta, \delta)$
 574 can be very wide in our setting and do not grant us much guidance. Therefore, it is best to compute some sort of
 575 empirical risk function based on data. All we have is past data, yet our goal is to compute future risk. We must
 576 forecast future data and then determine performance of our various options of decoy selection algorithms through
 577 forecast validation.

578 How to do forecasting and forecast validation? A naive, simple method to forecast future values is to assume
 579 that the values will be the same as in the current period. More sophisticated methods attempt to anticipate changes
 580 in the forecasted values by analyzing cycles and statistical dependence of the values. In our setting with multi-
 581 variate forecasting, some appropriate forecasting methods include Exponential Smoothing, Vector Autoregression
 582 (VAR), Vector Autoregressive Moving Average (VARMA), Generalized Autoregressive Conditional Heteroskedas-
 583 ticity (GARCH), and Kalman Filter.

584 Cross-validation is a popular general method to evaluate model accuracy. There are special considerations
 585 when the data is time series because time series data is not necessarily independent nor identically distributed.
 586 The general consensus in the academic literature is that when the characteristics of the time series are unknown
 587 then “out-of-sample” (OOS) cross-validation should be used. OOS cross-validation fits a forecasting model on

⁶<https://libera.monerologs.net/monero-research-lab/20220601#c103366>

588 all the data except the last few periods and then measures how well the model forecasts the data of the last few
 589 periods. OOS cross-validation is also known as “last block validation”, “forward validation”, and “holdout validation”
 590 ([Bergmeir & Benítez, 2012], [Cerqueira et al., 2020]).

591 To be specific, what I mean by “unknown” characteristics of a time series is that it is unknown whether the time
 592 series is stationary. Stationarity is a technical condition in time series that requires that its distribution does not
 593 depend on time. An independent and identically distributed series is stationary. A series that is neither independent
 594 nor identically distributed will not be stationary. Many financial time series are non-stationary. A common way to
 595 manage non-stationarity in data is to compute the first difference (or second difference if necessary, or third...), but
 596 it is not clear how this could be done when the object of observation is an entire distribution, as it is in our setting.

597 [Bergmeir et al., 2018] mathematically prove that standard K -fold cross-validation is a valid technique when
 598 the data series is stationary (plus a few other assumptions). They warn that K -fold cross-validation is not valid if
 599 the data series is non-stationary and show through Monte Carlo simulations that OOS validation performs better
 600 on non-stationary data. [Bergmeir & Benítez, 2012] arrive at a similar conclusion. [Cerqueira et al., 2020] separate
 601 dozens of real data sets into stationary and non-stationary and finds that “when the time series are non-stationary,
 602 the most accurate estimates are produced by out-of-sample methods, particularly the holdout approach repeated
 603 in multiple testing periods....When the observations in a data set are not i.i.d. [independently and identically
 604 distributed], the standard cross-validation approach is not directly applicable.” The top performing models in the
 605 M5 forecasting competition generally used the last 28 day period for cross-validation ([Makridakis et al., 2022]).

606 There is no particular reason to think that the spent output age distribution is stationary. Certainly, research
 607 into spent output age is in its infancy. Non-stationarity is the weaker assumption. To be “safe” it is better to impose
 608 fewer assumptions on statistical models if we cannot justify them. Furthermore, with only about 52 weeks of Monero
 609 data it would be difficult to perform a formal hypothesis test of stationarity with high statistical power. Therefore,
 610 it is best to use OOS cross-validation to evaluate forecast accuracy and risk. A form of OOS cross-validation is
 611 performed in the following section.

612 The `tsqsim` software created by Monero developer mj-xmr is capable of OOS cross-validation.⁷ Some modifi-
 613 cations will be necessary to support multivariate time series. Technically, spent output age is univariate, but since
 614 we are measuring the age *distribution* at each time period, it makes sense to model it in a multivariate way.

615 8 Inter-Temporal Stability of Spent Output Age Distribution for BTC, 616 BCH, LTC, and DOGE

617 Much like in **Section 5 Dry Run with Old Möser et al. (2018) Data**, it is useful to run an analysis of similar
 618 spent output age data from other blockchains to inform statistical modeling strategies.

619 The table below lists the share of payments made with several different cryptocurrencies with an unspent
 620 transaction output (UTXO) model. I ignored cryptocurrencies with an account model like Ethereum because the
 621 spending mechanism is fundamentally different. The main question that we want to answer is whether the chosen
 622 cryptocurrencies are used in a roughly similar manner to Monero: as peer-to-peer electronic cash. This table may
 623 suggest that BTC, BCH, LTC, and DOGE have somewhat similar usage as Monero. One major difference between
 624 these cryptocurrencies and Monero is that there is a 10 block lock enforced at the protocol level for Monero. BTC,
 625 BCH, LTC, and DOGE allow users to spend received funds immediately.

626

⁷<https://github.com/mj-xmr/tsqsim>

UTXO-based cryptocurrency usage as payment by percent (payment processors and merchants)							
	Service	Bitpay ⁸	CoinCards ⁹	Bitrefill ¹⁰	Cake Pay ¹¹	Travala ¹²	Shodan ¹³
	TXs/month	67,000	NA	186,000	NA	NA	220 total
	Time period	June 2022	July 2022	NA	Aug 2022	NA	NA
	Metric	Transactions	USD value	Unique users	USD value	Hotel nights	Subscriptions
627	BTC	53.3	41.0	40	16	9.2	47.3
	BCH	5.0	NA	NA	NA	0.5	4.1
	LTC	21.2	7.0	7	6	0.8	12.7
	DOGE	6.2	3.0	NA	NA	0.3	13.2
	XMR	NA	19.0	NA	78	1.9	NA
	DASH	NA	0.5	NA	NA	0.5	NA
	ADA	NA	NA	NA	NA	0.9	NA

628 In the next several section I perform statistical analysis of these four UTXO cryptocurrencies. The code is
 629 available at <https://github.com/Rucknium/OSPEAD/tree/main/General-Blockchain-Age-of-Spent-Outputs>. The
 630 code was executed on the Monero Research Computing Server, whose hardware was improved by a CCS proposal.¹⁴

631 8.1 Summary Characterization of Distributions Over Time

632 Figures 14 to 17 show several statistics about the age of spent outputs of BTC, BCH, LTC, and DOGE since 2015.
 633 The age units are in terms of blocks. For BTC and BCH the interval between blocks is 10 minutes. For LTC it
 634 is 2.5 minutes and for DOGE it is 1 minute. The unit of observation is the ISO week, a natural unit of economic
 635 time.¹⁵

636 The first line graphs show the mean, median, standard deviation, skewness, and kurtosis. The skewness and
 637 kurtosis statistics may be unfamiliar. They are the third and fourth standardized moments of a distribution,
 638 respectively. The moments of a distribution is defined by a power of the expectation $E[X]$, i.e. theoretical mean, of
 639 the distribution. The k th moment is $E[X^k]$. Moments extend the concept of moving from expectation to variance
 640 (which is the square of the standard deviation). The mean (expectation) of a random variable is simply the first
 641 moment:

$$\mu = E[X^1]$$

642 The variance is the second central moment:

$$\sigma^2 = E \left[(X - E[X])^2 \right]$$

643 The skewness is the third standardized moment (standardized by the standard deviation σ):

$$\tilde{\mu}_3 = E \left[\left(\frac{X - E[X]}{\sigma} \right)^3 \right]$$

644 The kurtosis is the fourth standardized moment:

⁸<https://bitpay.com/stats/>

⁹<https://twitter.com/CoinCards/status/1555286172385116164>

¹⁰<https://youtu.be/bkjEcSmZKfc?t=549>

¹¹<https://twitter.com/cakewallet/status/1565370179906838528>

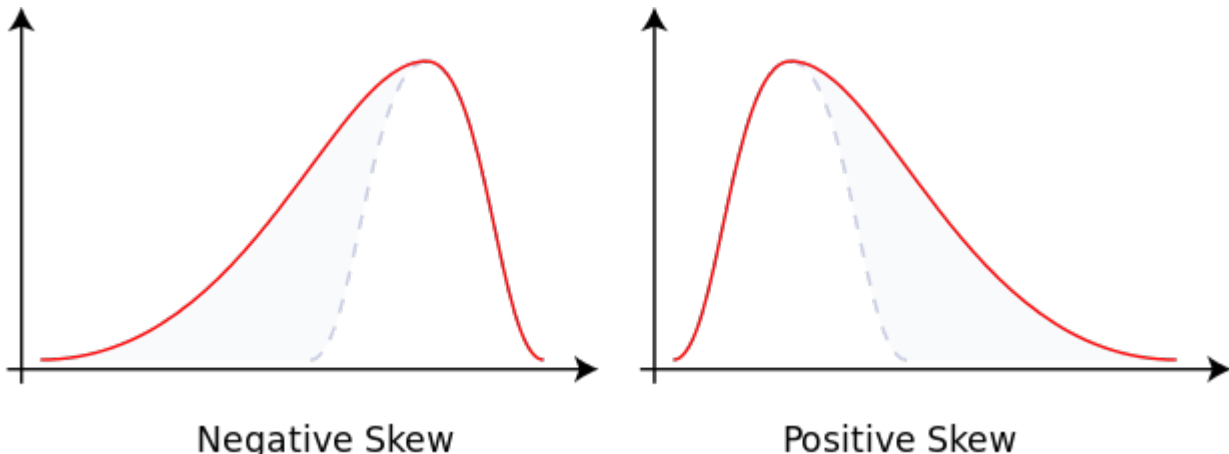
¹²<https://travala-dashboard.com/>

¹³<https://blog.shodan.io/accepting-crypto-a-vendor-perspective/>

¹⁴https://ccs.getmonero.org/proposals/gingeropolous_z zenith _storage.html

¹⁵https://en.wikipedia.org/wiki/ISO_week_date

Figure 13: Skewness



Source: [https://en.wikipedia.org/wiki/File:Negative_and_positive_skew_diagrams_\(English\).svg](https://en.wikipedia.org/wiki/File:Negative_and_positive_skew_diagrams_(English).svg)

$$\tilde{\mu}_4 = E \left[\left(\frac{X - E[X]}{\sigma} \right)^4 \right]$$

645 The mean is a measure of the central tendency of a distribution. The standard deviation is a measure of its
 646 dispersion (spread). The skewness and kurtosis of a distribution involve its characteristics in its tail or tails. A
 647 positive skew means that the distribution's tail is on the right side of the distribution. All the age distributions
 648 analyzed here tend to have a positive skew. High kurtosis means that large outliers are more likely. Kurtosis
 649 of greater than 3 suggests that a distribution has a fatter tail than the normal distribution. The skewness and
 650 kurtosis become relevant when very old outputs “wake up” during periods of exchange rate volatility to participate
 651 in speculative activity, i.e. buying and selling on exchanges.

652 The fitting function is essentially a minimum divergence estimator. This means that the parameters of the
 653 parametric probability density function (PDF) are chosen to minimize the distance between the parametric PDF
 654 and the PDF formed by the data (the empirical PDF), for some specified metric of “distance”.

655 There are several measures of distance that could be used. For the purpose of this exploration of output age
 656 distribution forecasting, the distance metric to be minimized will be the total linear sum of the mass of the estimated
 657 parametric PDF that falls below the empirical PDF. With the “loss function” specified this way, the optimization
 658 algorithm attempts to minimize the probability that the real spends are much more likely to come from a block of
 659 a particular age compared to a potential decoy. Ideally, the decoy distribution would be identical to the real spend
 660 age distribution, but parametric PDFs are not flexible enough to perfectly match an empirical PDF.

661 Define $f_S(x)$ as the empirical spent output age distribution at block age x and $f_D(x; \beta)$ as a potential “decoy”
 662 distribution with some parameter vector β (with the transparent blockchains presented here, there is no actual
 663 decoy mechanism of course). Then for each week of spent output age data the parameter vector β can be chosen
 664 to minimize this quantity:

$$L(\beta) = \sum_{i \in \{x_i : f_D(x_i; \beta) < f_S(x_i)\}}^N f_S(x_i) - f_D(x_i; \beta)$$

665 That is, minimize the sum of the difference between the real spend age distribution for blocks x_i where the decoy
 666 distribution is less than the real spend age distribution. The minimization is performed by computer numerical
 667 minimization methods similar to gradient descent.

668 The two candidate “decoy” parametric PDFs under consideration in this exercise are the Log-gamma (*lgamma*)

⁶⁶⁹ distribution and the Right-Pareto Log-normal (*rpln*) distribution. The lgamma distribution, with two parameters,
⁶⁷⁰ was used in [Möser et al., 2018] to suggest a decoy distribution that was later incorporated into Monero’s reference
⁶⁷¹ wallet software. The rpln distribution is a more flexible distribution, with three parameters. The PDFs of these
⁶⁷² two distributions are:

$$f_{lgamma}(x) = \frac{ratelog^{shapelog}}{\Gamma(shapelog)} \times \frac{(\ln x)^{shapelog-1}}{x^{ratelog+1}}$$

⁶⁷³ with $ratelog > 0$ and $shapelog > 0$ and where Γ is the gamma function and

$$f_{rpln}(x) = shape2 \times x^{-shape2-1} e^{shape2 \times meanlog + \frac{shape2^2 \times sdlog^2}{2}} \Phi\left(\frac{\ln x - meanlog - shape2 \times sdlog^2}{sdlog}\right)$$

⁶⁷⁴ with $shape2 > 0$ and $sdlog > 0$ and where Φ is the cumulative distribution function of the standard Normal
⁶⁷⁵ distribution.

Figure 14: BTC Summary Characterization of Spend Age Distribution Over Time

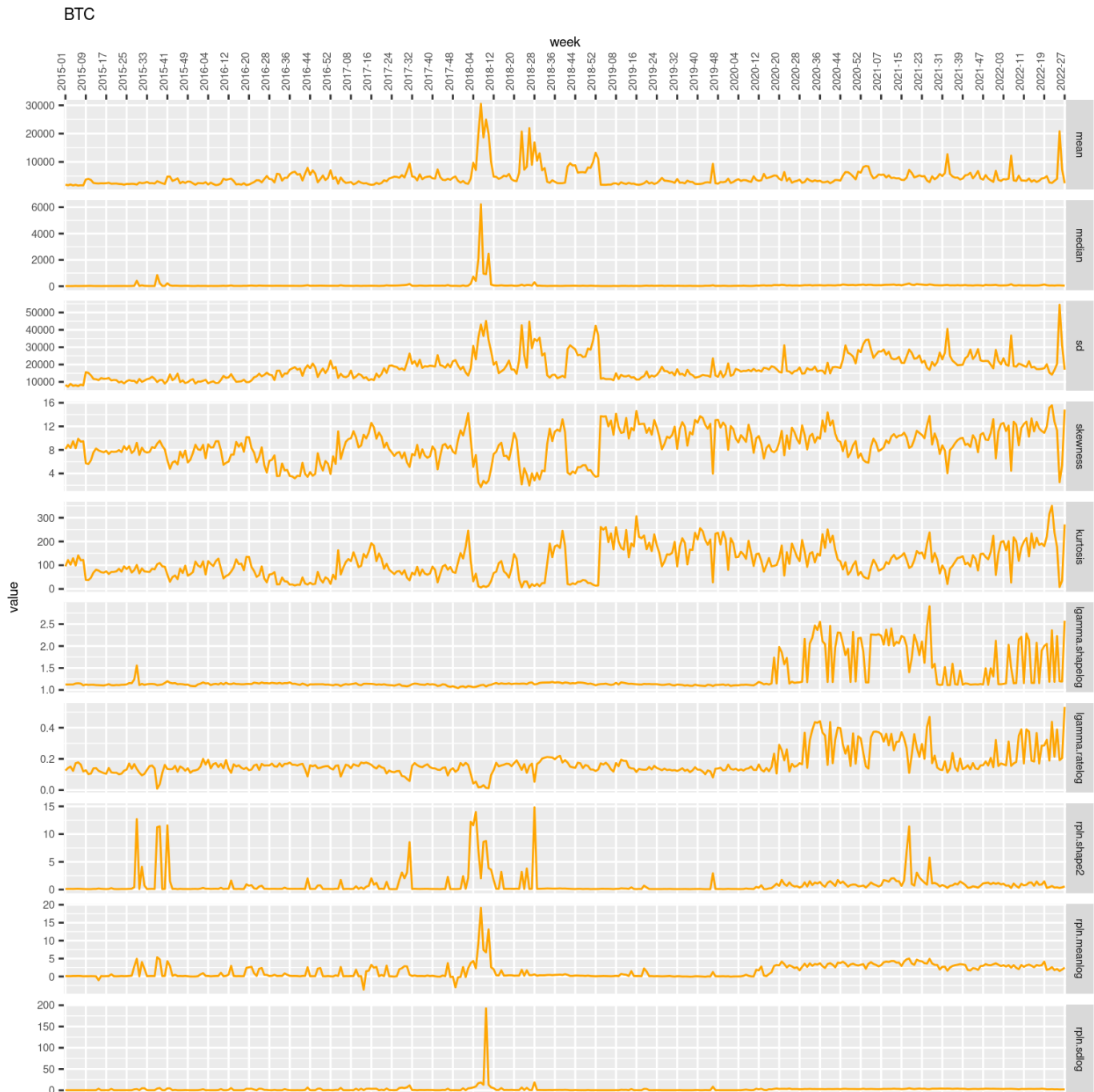


Figure 15: BCH Summary Characterization of Spend Age Distribution Over Time

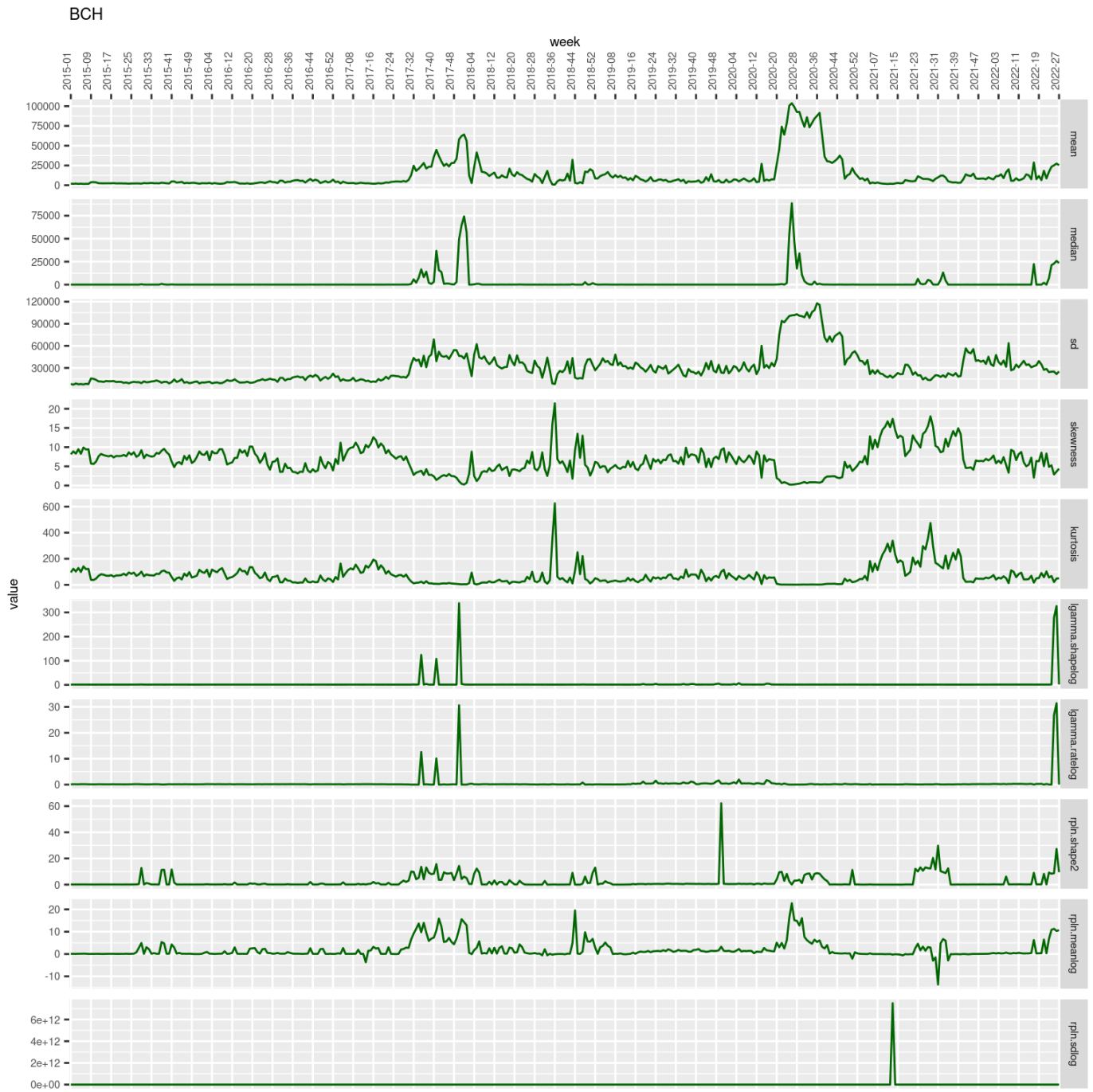


Figure 16: LTC Summary Characterization of Spend Age Distribution Over Time

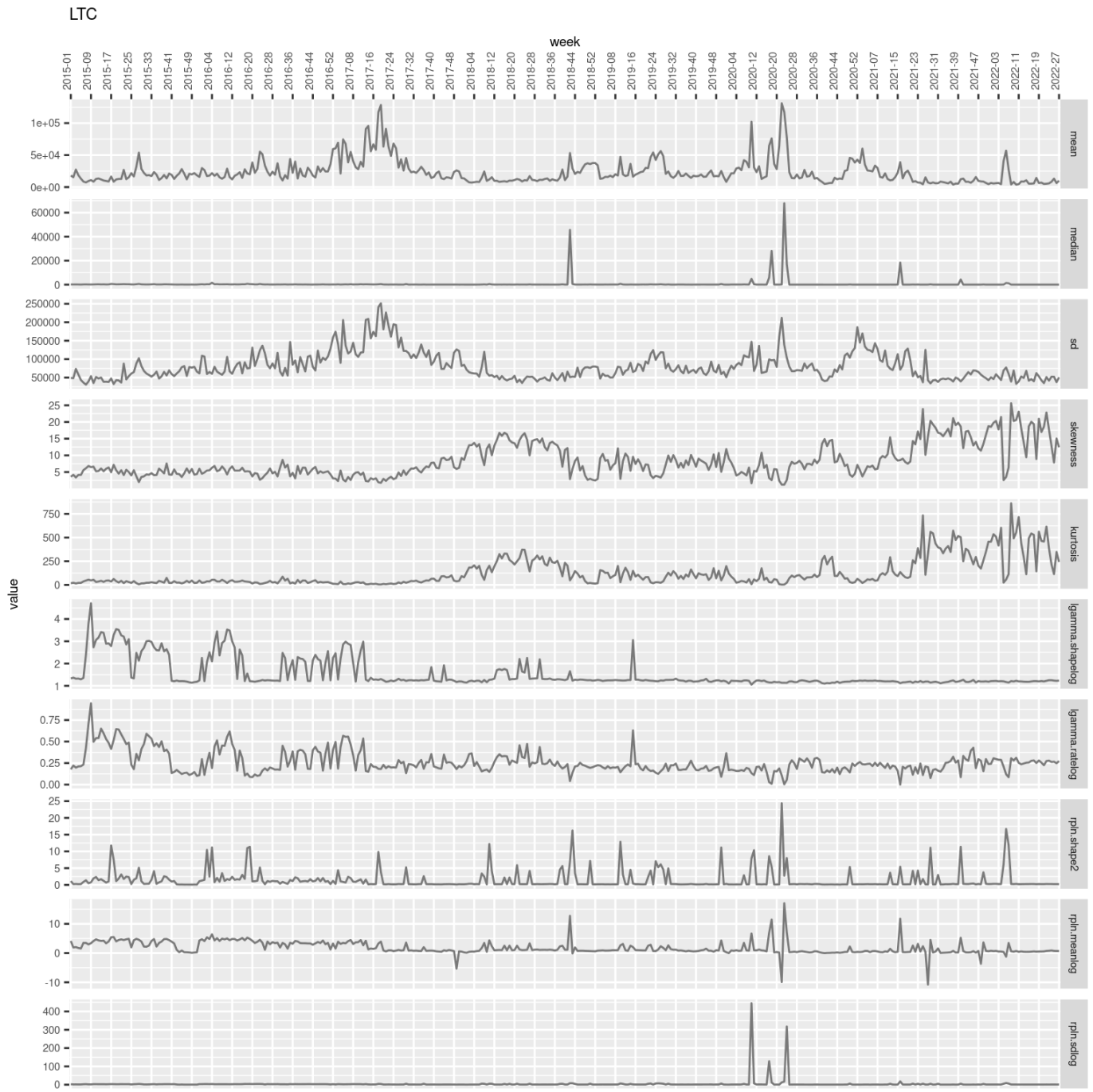
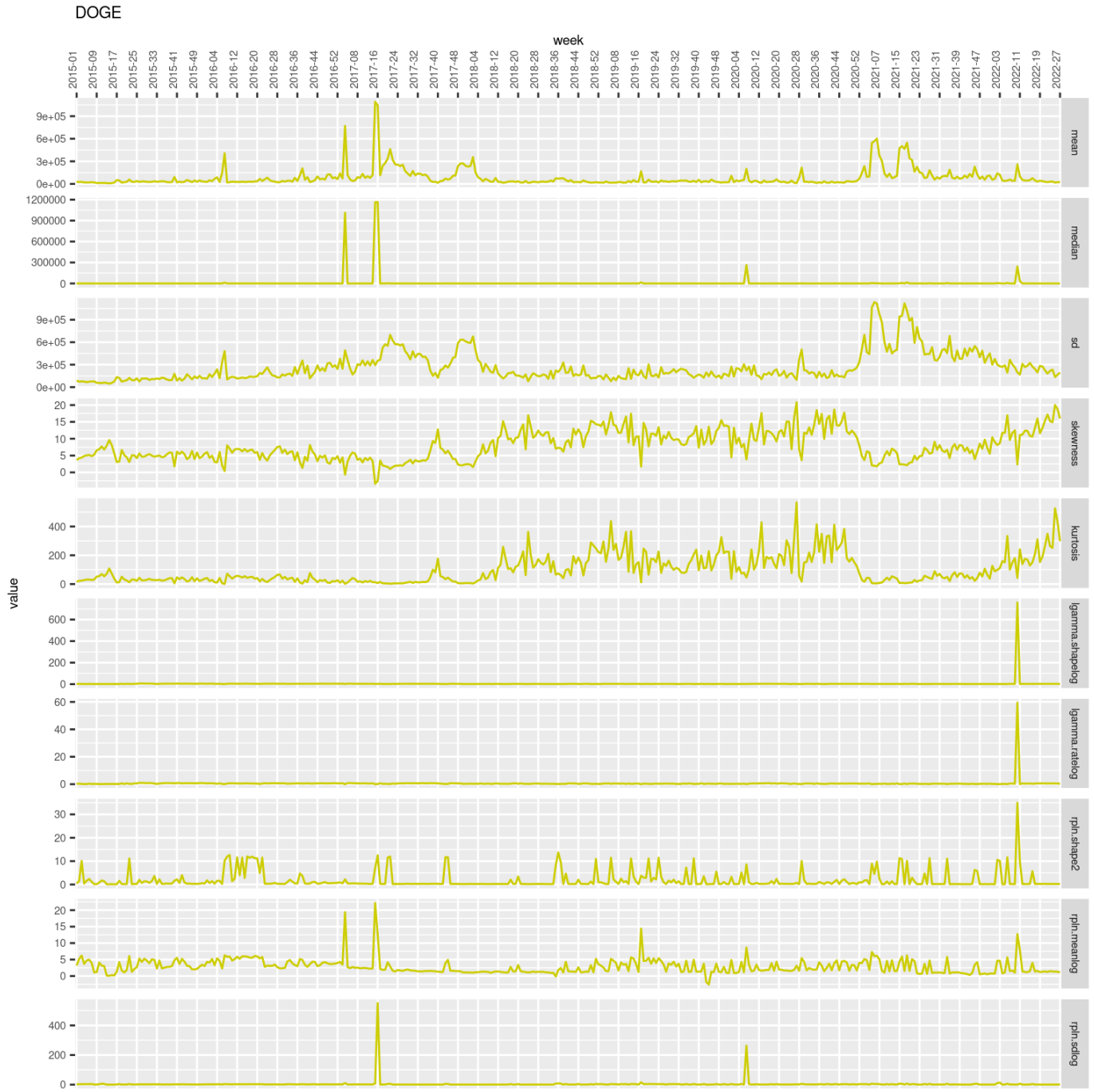


Figure 17: DOGE Summary Characterization of Spend Age Distribution Over Time



676 8.2 Cross-Blockchain Correlations of Summary Statistics Across Time

677 The following table contains the correlation between several statistics over time for each pair of blockchains. The
 678 “BTC&BCH” correlation included data only for January 2018 onward to avoid artificially raising the correlation by
 679 including weeks when the BTC and BCH contained the same transaction before the August 2017 hard fork.

680 To be precise, define vector $[x_{s,1}, x_{s,2}, \dots, x_{s,Z}] = \mathbf{X}_s$ for statistic s , e.g. the median, of blockchain x at each
 681 week, with Z total weeks in the sample. Define \mathbf{Y}_s for blockchain y similarly. Then the quantities displayed in
 682 Table 4 are $\text{corr}(\mathbf{X}_s, \mathbf{Y}_s)$.

683 The two statistics that tend to have consistently high correlation for each pair of blockchains are skewness and
 684 kurtosis.

Table 4: Cross-Blockchain Correlations of Summary Statistics Across Time

	BTC&BCH	BTC<C	BTC&DOGE	BCH<C	BCH&DOGE	LTC&DOGE
mean	-0.04	-0.04	-0.04	-0.01	-0.08	0.21
median	-0.03	-0.01	-0.01	-0.03	-0.02	-0.01
sd	-0.07	0.02	0.34	-0.02	0.02	0.35
skewness	0.09	0.24	0.19	0.11	-0.32	0.28
kurtosis	0.02	0.29	0.31	0.22	-0.26	0.23

685 8.3 Evaluation of Forecast Accuracy

686 OSPEAD needs to approximate the real spend age distribution in the future, not the past. Ideally, the decoy
 687 selection algorithm should mimic the real spend age distribution at the time that each transaction is made. Since
 688 the real spend age distribution is likely changing over time, some type of forecasting is needed. Here I perform some
 689 simple evaluation of forecasting methods on transparent blockchains.

690 Let W be the number of weeks in a forecast horizon. It is the approximate interval of time that a proposed
 691 decoy selection algorithm should aim to be accurate. Let M be the number of weeks in the data sample. Then a
 692 common way to evaluate a forecasting method is to use the first $M - W$ weeks to fit a forecasting model. Then
 693 determine the performance of the method by forecasting for W weeks into the “future” and compare with the actual
 694 sample data of the final W weeks. This is known as out-of-sample validation. For this exercise, I set $W = 8$.

695 An entire distribution needs to be forecast rather than a single value or a set of values. Forecasting an entire
 696 (empirical, nonparametric) distribution is extremely complex, so here I reduce the magnitude of the forecasting
 697 problem to just the parameters of the fitted parametric distributions (lgamma and rpln).

698 As an initial test, the sophisticated forecasting method used here was a multivariate auto-regressive(1) exoge-
 699 nous inputs state-space model with a Koopman-Durbin Kalman filter implemented in the MARSS R package. The
 700 forecasting method allows a forecast into each period in the future. Since the “S” in OSPEAD stands for “Static”,
 701 only one of the forecast periods can be chosen. I chose the 4th forecast period since it is roughly in the middle of
 702 the 8-week forecast horizon. This forecast is referred to as simply `forecast.accuracy` below.

703 I also evaluated two naive forecasting methods. The first is to use the parameters of the $M - W$ th week, i.e. the
 704 last week of the “training set”, as the forecast. This is called `forecast.accuracy.naive.final.week` below. The
 705 second naive method (`forecast.accuracy.naive.horizon.period`) is to use the final W weeks of the training set
 706 to fit the specified lgamma and rpln distributions by minimizing the $L(\beta)$ loss function for a set of weeks of data
 707 pooled together rather than a single week.

708 Given that the loss function $L(\beta)$ is not globally convex in the choice parameters β , the numerical optimization
 709 algorithm can go “off the rails” and settle at a local rather than global minimum. Such a failure mode is especially
 710 likely if the empirical distribution is unusual or if the starting values given to the optimization algorithm are far from
 711 the global minimum. Generally, the solution to this problem is to try different optimization algorithms, determined
 712 better starting values, or use a computationally expensive grid search method. I chose to defer dealing with the
 713 issue to a later stage in the process. For the purposes of forecasting, I removed any weeks where the estimated
 714 parameters of the parametric distributions were greater than (or less than) five times the 95th (5th) percentile from
 715 the median. For example, this exclusion step caused the forecast evaluation for BCH to use the 15th through 24th
 716 weeks of 2022 rather than the 20th through 27th week as for other blockchains.

717 The results of the forecast evaluation are in Table 5. Forecasts were evaluated based on the value of their loss
 718 function $L(\beta)$ for each out-of-sample week. Lower values indicate better performance. The minimum possible value

719 is 0 and the maximum possible value is 1. The color code scales were calculated separately for each blockchain.
720 Each color claims a value bin of equal size. Higher values are red, average values are yellow, and low values are
721 green.

722 In this preliminary exercise, `rpln.forecast.accuracy.naive.horizon.period` appears to have the most con-
723 sistently good performance across blockchains.

Table 5: Evaluation of forecast accuracy

		BTC		BCH		LTC		DOGE															
	rownames	mean	sd	2022-20	2022-21	2022-22	2022-23	2022-24	2022-25	2022-26	2022-27												
rphn_forecast_accuracy	0.1225	0.0294	0.0952	0.1086	0.1058	0.1227	0.0926	0.1814	0.1319	0.1421													
rphn_forecast_accuracy_naive_final_week	0.1213	0.0295	0.0951	0.1068	0.1037	0.1222	0.0910	0.1807	0.1313	0.1397													
rphn_forecast_accuracy_naive_horizon_period	0.0682	0.0244	0.0795	0.0504	0.0541	0.0601	0.0501	0.1237	0.0645	0.0632													
lgamma_forecast_accuracy	0.1256	0.0215	0.1216	0.1103	0.1151	0.1149	0.1059	0.1733	0.1299	0.1341													
lgamma_forecast_accuracy_naive_final_week	0.1495	0.0277	0.1179	0.1373	0.1373	0.1519	0.1188	0.1996	0.1613	0.1717													
lgamma_forecast_accuracy_naive_horizon_period	0.1338	0.0177	0.1302	0.1183	0.1274	0.1212	0.1205	0.1716	0.1358	0.1453													
		rownames		mean		sd		2022-15		2022-16		2022-18		2022-19		2022-20		2022-21		2022-22		2022-24	
		rphn_forecast_accuracy		0.2416		0.1923		0.1811		0.1420		0.1147		0.1598		0.1057		0.4079		0.1665		0.6547	
		rphn_forecast_accuracy_naive_final_week		0.2452		0.1808		0.1882		0.1530		0.1302		0.1668		0.1208		0.3957		0.1692		0.6375	
		rphn_forecast_accuracy_naive_horizon_period		0.3938		0.0463		0.3837		0.3886		0.3754		0.3830		0.3809		0.3812		0.3526		0.5051	
		lgamma_forecast_accuracy		0.3654		0.1374		0.2606		0.2757		0.2574		0.3479		0.2506		0.3830		0.5578		0.5906	
		lgamma_forecast_accuracy_naive_final_week		0.3573		0.1491		0.2401		0.2553		0.2367		0.3476		0.2313		0.3867		0.5643		0.5967	
		lgamma_forecast_accuracy_naive_horizon_period		0.4179		0.0769		0.3675		0.3757		0.3720		0.3858		0.3473		0.4209		0.5200		0.5539	
		rownames		mean		sd		2022-20		2022-21		2022-22		2022-23		2022-24		2022-25		2022-26		2022-27	
		rphn_forecast_accuracy		0.0950		0.0182		0.0736		0.0849		0.0718		0.1054		0.1139		0.1184		0.0859		0.1060	
		rphn_forecast_accuracy_naive_final_week		0.0947		0.0183		0.0748		0.0864		0.0691		0.1036		0.1123		0.1197		0.0859		0.1059	
		rphn_forecast_accuracy_naive_horizon_period		0.0883		0.0150		0.0762		0.0827		0.0682		0.0951		0.1015		0.1108		0.0745		0.0974	
		lgamma_forecast_accuracy		0.1112		0.0181		0.0873		0.1014		0.0899		0.1231		0.1328		0.1317		0.1035		0.1201	
		lgamma_forecast_accuracy_naive_final_week		0.1120		0.0181		0.0880		0.1025		0.0906		0.1239		0.1336		0.1324		0.1044		0.1208	
		lgamma_forecast_accuracy_naive_horizon_period		0.1056		0.0162		0.0853		0.0949		0.0893		0.1168		0.1247		0.1248		0.0949		0.1144	
		rownames		mean		sd		2022-20		2022-21		2022-22		2022-23		2022-24		2022-25		2022-26		2022-27	
		rphn_forecast_accuracy		0.2410		0.0202		0.2446		0.2479		0.2635		0.2692		0.2431		0.2137		0.2300		0.2161	
		rphn_forecast_accuracy_naive_final_week		0.1928		0.0203		0.2044		0.2070		0.2104		0.2179		0.1903		0.1626		0.1799		0.1697	
		rphn_forecast_accuracy_naive_horizon_period		0.1888		0.0199		0.2089		0.2049		0.1995		0.2100		0.1786		0.1548		0.1773		0.1761	
		lgamma_forecast_accuracy		0.2093		0.0177		0.2329		0.2231		0.2186		0.2154		0.1935		0.1770		0.2037		0.2106	
		lgamma_forecast_accuracy_naive_final_week		0.2050		0.0174		0.2139		0.2153		0.2205		0.2262		0.2012		0.1728		0.1967		0.1934	
		lgamma_forecast_accuracy_naive_horizon_period		0.1953		0.0177		0.2127		0.2091		0.2040		0.2125		0.1859		0.1619		0.1904		0.1856	

724 8.4 Animated Evolution of Distributions

725 I created gif animations of the empirical probability densities of each blockchain's spent output age distribution over
 726 time. The green line is the current week's empirical density, with faint echoes of prior weeks in other colors. The
 727 fitted lgamma distribution line is white and rpln is red. The horizontal axis of the first charts for each blockchain
 728 has a log scale. Both the horizontal and vertical charts are log scale for the second chart of each blockchain. The
 729 "1" on the horizontal axis should be interpreted as "0". In other words, a "1" means that the age of the spent output
 730 is approximately zero. This would occur if (1) a child transaction spent an output from a parent transaction that
 731 was confirmed in the same block as the child transaction; (2) the timestamps of blocks were out of order, leading
 732 to a "negative" age; (3) the block was confirmed at a time interval less than half of the target block time, e.g. 5
 733 minutes for BTC/BCH, leading to rounding down to zero.

734 There is a clear daily cycle visible in the log-log scale charts.

735 To view the animated gifs, visit:

736 <https://rucknium.me/html/spent-output-age-btc-bch-ltc-doge.html>

737 9 Options for Forecasting

738 My suggestion is to reduce the dimensionality of the forecasting problem by forecasting the parameters of parametric
 739 distributions, as in **Section 8.3 Evaluation of Forecast Accuracy**. In this case we would need forecasting
 740 methods that can handle multivariate forecasting objectives. Beyond that requirement, there are few theoretical
 741 reasons to favor particular forecasting methods in this setting. Out-of-sample forecasting validation should guide
 742 the final choice of forecast method. The one exception is forecasting methods that technically require the time
 743 series to be stationary. We may want to somewhat discount such methods and choose one only if it offers much
 744 superior performance to a method that allows non-stationarity.

745 Forecasting methods under consideration include:

- 746 1. Exponential Smoothing. The `legion` R package can perform multivariate Exponential Smoothing.
 - 747 2. Vector Autoregression (VAR). The `MTS` R package can perform VAR forecasting through its `VARpred` function.
 748 Note that VAR generally requires stationary time series unless explicit cointegration relationships are specified
 749 as in a Vector Error Correction model.
 - 750 3. Vector Autoreregressive Moving Average (VARMA). The `MTS` R package can perform VAR forecasting through
 751 its `VARMAPred` function. Generally, stationarity is required.
 - 752 4. Generalized Autoregressive Conditional Heteroskedasticity (GARCH). The `rmgarch` R package offers multi-
 753 variate GARCH forecasting. Generally, stationarity is required.
 - 754 5. Kalman Filter. The `MARSS` and `KFAS` R packages provide multivariate Kalman Filter forecasting methods.
 - 755 6. A naive forecast where the forecast is just the value of the parameters of the last period in the training set.
 - 756 7. A naive forecast where the parameters are fit on multiple weeks of pooled data on the last part of the training
 757 set.
- 758 A simple way to evaluate forecast accuracy is to compute the loss function on some final W number of weeks as
 759 I did in **Section 8.3 Evaluation of Forecast Accuracy**. Another option is to perform the evaluation on a
 760 rolling window, called "evaluation on a rolling forecasting origin" in Section 5.10 "Time series cross-validation" of
 761 [Hyndman & Athanasopoulos, 2021]. For now for notational simplicity we will assume the former method.

Let \mathcal{Q} be the set of forecasting methods listed above and $q(\beta)$ be a particular element of the \mathcal{Q} set. $q(\beta)$ is a function that takes as arguments fitted parameter values $\hat{\beta}$ of parametric PDFs $f(x|\beta) \in \mathcal{F}$ of past weekly values and outputs forecasts $\tilde{\beta}$ for future β . Considering the fitting procedure from Equation (13), the final decoy selection algorithm parametric distribution $f(x|\beta)$ and parameters β should be chosen by:

$$\arg \min_{f(x|\beta) \in \mathcal{F}, q(\hat{\beta}) \in \mathcal{Q}} \frac{1}{W} \sum_{i=1}^W L\left(f\left(x_i \mid q\left(\hat{\beta}\right)\right)\right), \forall q \in \mathcal{Q} \quad (14)$$

Expression (14) will find the minimizers $f(x|\tilde{\beta})$ of each loss function $L \in \mathcal{L}$ among all parametric distributions $f(x|\beta) \in \mathcal{F}$ and all forecasting methods $q(\beta) \in \mathcal{Q}$ of the mean for the out-of-sample data x_i for weeks $i = 1, \dots, W$. Once these $f(x|\tilde{\beta})$ are found, the only decision left to be made is the judgment call on the proper choice of loss function and any associated loss function parameters λ, α, η . For example, in Table 5, Expression (14) would choose `rpln.forecast.accuracy.naive.horizon.period` for BTC, LTC, and DOGE, and `rpln.forecast.accuracy` for BCH. Note that Expression (14) forms a plug-in estimator for the risk function in Equation (2). Therefore, it is a type of empirical risk minimizer.¹⁶

10 Acknowledgments

This research was funded by Monero's Community Crowdfunding System:

<https://ccs.getmonero.org/proposals/Rucknium-OSPEAD-Fortifying-Monero-Against-Statistical-Attack.html>

The following people gave feedback on the research process and/or contributed in other ways: ACK-J, ArcticMine, bob, coinstudent2048, garth, gingeropolous, isthmus, jberman, kayabaNerve, koe, mj-xmr, monerobull, moneromooo, neptune, plowsof, SamsungGalaxyPlayer, SerHack, SethForPrivacy, and Syksy.

¹⁶https://en.wikipedia.org/wiki/Empirical_risk_minimization#Empirical_risk_minimization

779 References

- 780 [Bergmeir & Benítez, 2012] Bergmeir, C. & Benítez, J. M. (2012). On the use of cross-validation for time series
781 predictor evaluation. *Information Sciences*, 191, 192–213. <https://doi.org/https://doi.org/10.1016/j.ins.2011.12.028>. Data Mining for Software Trustworthiness
- 783 [Bergmeir et al., 2018] Bergmeir, C., Hyndman, R. J., & Koo, B. (2018). A note on the validity of cross-validation
784 for evaluating autoregressive time series prediction. *Computational Statistics & Data Analysis*, 120, 70–83.
785 <https://doi.org/https://doi.org/10.1016/j.csda.2017.11.003>
- 786 [Casella & Berger, 2002] Casella, G. & Berger, R. L. (2002). *Statistical Inference* (second ed.). Duxbury Pacific
787 Grove, CA.
- 788 [Cerqueira et al., 2020] Cerqueira, V., Torgo, L., & Mozetič, I. (2020). Evaluating time series forecasting models:
789 an empirical study on performance estimation methods. *Machine Learning*, 109(11), 1997–2028. <https://doi.org/10.1007/s10994-020-05910-7>
- 791 [Creedy, 2015] Creedy, J. (2015). A Note on Computing the Gini Inequality Measure with Weighted Data. Working
792 Paper Series 4235, Victoria University of Wellington, Chair in Public Finance. <https://ideas.repec.org/p/vuw/vuwcpf/4235.html>
- 794 [Hsu et al., 2014] Hsu, J., Gaboardi, M., Haeberlen, A., Khanna, S., Narayan, A., Pierce, B. C., & Roth, A. (2014).
795 Differential privacy: An economic method for choosing epsilon. *2014 IEEE 27th Computer Security Foundations
796 Symposium*. <https://doi.org/10.1109/csf.2014.35>
- 797 [Hyndman & Athanasopoulos, 2021] Hyndman, R. J. & Athanasopoulos, G. (2021). *Forecasting: Principles and
798 Practice* (third ed.). OTexts: Melbourne, Australia. <https://otexts.com/fpp3/>
- 799 [Krawiec-Thayer et al., 2021] Krawiec-Thayer, M. P., Neptune, Rucknium, Jberman, &
800 Carrington (2021). *Fingerprinting a flood: forensic statistical analysis of the
801 mid-2021 monero transaction volume anomaly*. <https://mitchellpkt.medium.com/fingerprinting-a-flood-forensic-statistical-analysis-of-the-mid-2021-monero-transaction-volume-a19cbf41ce60>
802 Available at <https://mitchellpkt.medium.com/fingerprinting-a-flood-forensic-statistical-analysis-of-the-mid-2021-monero-transaction-volume-a19cbf41ce60>
- 805 [Kumar et al., 2017] Kumar, A., Fischer, C., Tople, S., & Saxena, P. (2017). A traceability analysis of monero's
806 blockchain. *European Symposium on Research in Computer Security (ESORICS)*. https://doi.org/10.1007/978-3-319-66399-9_9
- 808 [Mackenzie et al., 2015] Mackenzie, A., Noether, S., & Team, M. C. (2015). *Improving obfuscation in the cryptonote
809 protocol*. Research Bulletin. <https://www.getmonero.org/resources/research-lab/pubs/MRL-0004.pdf>
- 810 [Maji et al., 2019] Maji, A., Ghosh, A., Basu, A., & Pardo, L. (2019). Robust statistical inference based on the
811 c-divergence family. *Annals of the Institute of Statistical Mathematics*, 71(5), 1289–1322. <https://doi.org/10.1007/s10463-018-0678-5>
- 813 [Makarov & Schoar, 2021] Makarov, I. & Schoar, A. (2021). Blockchain analysis of the bitcoin market. Working
814 Paper 29396, National Bureau of Economic Research. <https://doi.org/10.3386/w29396>
- 815 [Makridakis et al., 2022] Makridakis, S., Spiliotis, E., & Assimakopoulos, V. (2022). M5 accuracy competition:
816 Results, findings, and conclusions. *International Journal of Forecasting*. <https://doi.org/https://doi.org/10.1016/j.ijforecast.2021.11.013>
- 818 [Möser et al., 2018] Möser, M., Soska, K., Heilman, E., Lee, K., Heffan, H., Srivastava, S., Hogan, K., Hen-
819 nessey, J., Miller, A., Narayanan, A., & Christin, N. (2018). An empirical analysis of traceability in the mon-
820 ero blockchain. *Proceedings on Privacy Enhancing Technologies*, 2018(3), 143–163. <https://doi.org/doi:10.1515/popets-2018-0025>
- 822 [Reed & Jorgensen, 2004] Reed, W. J. & Jorgensen, M. (2004). The double pareto-lognormal distribution—a new
823 parametric model for size distributions. *Communications in Statistics - Theory and Methods*, 33(8), 1733–1753.
824 <https://doi.org/10.1081/STA-120037438>

- 825 [Ronge et al., 2021] Ronge, V., Egger, C., Lai, R. W. F., Schröder, D., & Yin, H. H. F. (2021). Foundations
826 of ring sampling. *Proceedings on Privacy Enhancing Technologies*, 2021(3), 265–288. <https://doi.org/doi:10.2478/popets-2021-0047>
- 828 [Vijayakumaran, 2021] Vijayakumaran, S. (2021). *Analysis of cryptonote transaction graphs using the dulmage-*
829 *mendelsohn decomposition*. Cryptology ePrint Archive, Report 2021/760. <https://eprint.iacr.org/2021/760>
- 830 [Ye et al., 2020] Ye, C., Ojukwu, C., Hsu, A., & Hu, R. (2020). *Alt-coin traceability*. Cryptology ePrint Archive,
831 Report 2020/593. <https://eprint.iacr.org/2020/593>